In Situ Direct Sampling Mass Spectrometric Study on Formation of Polycyclic Aromatic Hydrocarbons in Toluene Pyrolysis

Bikau Shukla, Akio Susa, Akira Miyoshi, and Mitsuo Koshi*

Department of Chemical System Engineering, The University of Tokyo, 7-3-1 Bunkyo-ku, Hongo, Tokyo 113-8656, Japan

Received: March 6, 2007; In Final Form: May 31, 2007

The gas-phase reaction products of toluene pyrolysis with and without acetylene addition produced in a flow tube reactor at pressures of 8.15−15.11 Torr and temperatures of 1136−1507 K with constant residence time (0.56 s) have been detected in an in situ direct sampling mass spectrometric study by using a vacuum ultraviolet single-photon ionization time-of-flight mass spectrometry technique. Those products range from methyl radical to large polycyclic aromatic hydrocarbons (PAHs) of mass 522 amu ($C_{42}H_{18}$) including smaller species, radicals, polyynes, and PAHs, together with ethynyl, methyl, and phenyl PAHs. On the basis of observed mass spectra, the chemical kinetic mechanisms of the formation of products are discussed. Especially, acetylene is mixed with toluene to understand the effect of the hydrogen abstraction and acetylene addition (HACA) mechanism on the formation pathways of products in toluene pyrolysis. The most prominent outputs of this work are the direct detection of large PAHs and new reaction pathways for the formation of PAHs with the major role of cyclopenta-fused radicals. The basis of this new reaction route is the appearance of different sequences of mass spectra that well explain the major role of aromatic radicals mainly cyclopenta fused radicals of PAHs resulting from their corresponding methyl PAHs, with active participation of c-C_5H_5, C_6H_5, $C_6H_5CH_2$, and C_9H_7 in the formation of large PAHs. The role of the HACA only seemed important for the formation of stable condensed PAHs from unstable primary PAHs with zigzag structure (having triple fusing sites) in one step by ring growth with two carbon atoms.

Introduction

The study of soot precursors, carbonaceous nanoparticles (NPs), and polycyclic aromatic hydrocarbons (PAHs; precursor of NP), which are produced in many practical combustion systems such as diesel engines and spark ignition engines, is a hot and interesting research topic in combustion, environmental, and health research due to their technological, environmental, health, and economical impacts. Though, more than a century of continuous research in combustion[1] experimental and modeling studies seemed to coincide at the concept of coagulation of precursors for soot formation. However, until now, no attempt has been successful to propose the final chemical precursor and the stage at which they start to coalesce. It is widely accepted that gaseous precursors that coagulate into the first soot particle are PAHs,[2−7] because (i) it bridges the mass gap between hydrocarbon fuel and soot and (ii) the chemical structure of soot is similar to PAH on an atomic level, i.e., a honeycomb-like network of sp^2 carbons. The generation process of final PAHs in terms of chemical kinetic mechanism is still not perfectly understood. Still unanswered questions are at what stage the coagulation commences and what form it takes.[8] Many studies forwarded pyrene as a final aromatic precursor[8−11] while some studies believed coronene[12] instead of pyrene. Recently, it again becomes a subject of discussion among the combustion scientists that whether coronene (300 amu) is sufficient for coagulation into the very high mass of the first soot particle (~2000 amu) or not as some recent studies[13−16] have detected

many PAHs greater than coronene. Thus, the formation mechanism of PAHs and soot[7] still remains challenging in the area of oxidation and pyrolysis of hydrocarbon fuels.

The kinetic mechanism of aliphatic hydrocarbon combustion is widely developed up to pyrene[9] although it needs to be modified so that it includes the mechanism for the formation of the large PAHs based on experimental and modeling results as recent studies[14,15,17−19] have already detected large PAHs. However, the kinetic mechanism for the formation of PAHs in aromatic hydrocarbon combustion and pyrolysis is poorly understood. Marsh et al.[20] have detected 3−10-ring PAHs in benzene droplet combustion by using high-perfromance liquid chromatography (HPLC) and UV absorption spectroscopy, but they have not reported any kinetic mechanism for the formation of those PAHs.

Toluene becomes our first choice due to its importance. It is itself toxic and produces many toxic PAHs and carbonaceous nanoparticles during its pyrolysis and oxidation. It is the most abundant component of the majority of practical fuels. For example, jet fuels and gasoline contain 20−30% toluene by mole fraction, due to its high energy density and anti-knocking capacity. It is also produced during the oxidation of other hydrocarbons and commercial fuels. Toluene pyrolysis is very important to understand the decomposition of all alkylated aromatic hydrocarbons as it involves two different channels of bond fissions, i.e., C−H bond fission, which produces benzyl and hydrogen radicals, and C−C bond fission, which produces phenyl and methyl radicals. Research on toluene pyrolysis has been concentrated on two major objectives: (a) determination of rate constants for toluene decomposition channels,[10,21−34] (b)

* Author to whom correspondence should be addressed. Phone: +81-3-5841-7295. Fax: +81-3-5841-7488. E-mail: koshi@chemsys.t.u-tokyo.ac.jp.

PAH Formation in Toluene Pyrolysis

J. Phys. Chem. A, Vol. 111, No. 34, 2007 **8309**

identification of gas-phase reaction products up to PAHs and investigation of their formation mechanisms.[10,22,27,30,31,35−40] Although the first part has been studied in detail, the second part is still unclear due to a lack of on-line results. Some studies also aimed to observe toluene oxidation products[41−47] but oxidation of toluene also suffers from a lack of on-line results for gas-phase reaction products up to large PAHs. Among the theoretical studies, Sivaramakrishnan et al.[48,49] focused on modeling of kinetic behaviors of $C_6H_5CH_3$, CH_4, C_2H_2, C_4H_2, C_6H_6, C_8H_6, and C_9H_8 from experimental[21,26,48] and theoretical data.[50] Agafonov et al.[51] reported a kinetic model including small PAHs, only suitable for smaller species in shock tube pyrolysis and oxidation of toluene. Among the experimental studies, Pamidimukkala et al.[22] observed only the smaller species C_2H_2, C_4H_2, and CH_4, and Colket et al.[10] observed PAH products up to pyrene. Studies of toluene pyrolysis by Smith et al.[30,31] are the only on-line attempts to observe the product species up to A_5 ($C_{20}H_{12}$) by using a Knudsen cell coupled to a mass spectrometer at high temperatures and very low pressures. Mathieu et al.[13] have observed mass signals up to 570 amu as desorbed species from soot particles with contamination of Na and K and have not forwarded any formation mechanism for those PAHs.

Until now, almost all attempts made to investigate this very complex issue were by indirect methods, i.e., gas chromatography, liquid chromatography, or HPLC with mass spectrometry, called the "preconcentration method", i.e., by trapping the exhaust molecules on a suitable adsorbent which are further separated by pretreatment (i.e., extraction). This method is time-consuming and excludes direct real-time in situ analysis. It is only suitable for stable species and does not provide any information about radicals, which are key species for developing the mechanism. The shock tube technique[13,21,22,25−27,39,48,49] has been used for the thermal unimolecular decomposition of toluene, and some studies[10,22,23,30,31,34,38] include the product observation up to PAHs. Mathieu et al.[13] has used laser desorption ionization (LDI) time-of-flight mass spectrometry (TOFMS), which cannot detect lower aliphatic and aromatic species. Only a few on-line results[30,31,52] were reported by using mass spectrometry.

This overview of previous studies clearly shows the necessity of direct identification of gas-phase reaction products up to large PAHs and motivated us to observe the products of toluene pyrolysis by a direct experiment to clarify the whole mechanism. The main objective of our research is the direct observation of PAHs higher than coronene to fulfill the gap between coronene and the first soot particle as shown in the soot model[12] to clarify the PAH generation mechanism based on on-line experimental results. The present work has determined the dominant reaction pathways for the formation of all identified products under the present experimental conditions as the first step of our final goal to develop the soot generation mechanism.

Experimental Section

In situ detection of the soot precursor in hydrocarbon combustion and pyrolysis needs a selective and sensitive analytical method. The most promising one for instrumental analytical purposes is the TOFMS with a selective and soft (fragment-free) ionization technique. The production of VUV radiation to achieve single-photon ionization (SPI) and TOFMS proved to be a powerful and useful technique for on-line detection of gas-phase species. This technique has already been successfully used by some studies[53−56] for detection of gas-phase products.

A schematic of the experimental setup is shown in Figure 1. The apparatus consists of a vacuum (source) chamber and

Figure 1. Experimental setup consisting of a quartz reaction tube and VUV-SPI-TOFMS.

detection (TOFMS) chamber separated from each other by a gate valve. A quartz reaction tube ($\Phi = 14$ mm, length $= 56$ cm) having a pinhole ($\Phi = 0.15$ mm) in the center was fixed in the source chamber with careful alignment of the pinhole on the center line of the skimmer of the TOFMS. The pinhole area of the reactor was wrapped with a tungsten heater (coil length $= 22$ cm). The heater was covered (leaving the pinhole uncovered) with two other pieces of quartz tubes ($\Phi = 18$ mm) wrapped with the Ni foil to avoid heat loss by radiation. To measure the temperature of the reaction, a K-type thermocouple ($\Phi = 0.65$ mm) was introduced into the reaction tube from the downstream. The typical pressure of the source chamber was kept at 2.8×10^{-8} Torr, and that of the TOF chamber was kept at 4.1×10^{-7} Torr, respectively, before each experimental run. A third harmonic UV laser pulse (355 nm) generated by a frequency conversion of a Nd:YAG laser (Surelite SSP Continuum) was focused by a quartz lens ($f = 150$ mm) and passed through the quartz window into the 13 cm SUS tube, the frequency tripling cell, filled with a nonlinear medium xenon (pressure $= 7.40$ Torr) for tripling the UV laser pulse at 355 nm into the VUV photon at 118 nm (10.5 eV). The UV (355 nm) and VUV (118 nm) beams were separated by a LiF crystal prism to avoid the fragmentation of the product molecules (due to the $(1 + 1)$ ionization by 355 and 118 nm photons). The 355 nm pulses was dumped on the inner wall of the tripling tube and only 118 nm photons were allowed to strike the molecular beam in the ionization region of the mass spectrometer to ionize all species having an ionization potential (IP) less than 10.5 eV. The ion source and flight tube were differently pumped by 1600 and 500 L/s turbo-molecular pumps followed by rotary pumps.

At first temperature profiles were taken to fix the position of the thermocouple for measuring the reaction temperature; 40% toluene and 60% He in the case of only toluene pyrolysis and 20% toluene, 20% acetylene, and 60% He in the case of toluene and acetylene mixture were supplied through mass flow controllers into the quartz reaction tube. The gaseous product molecules were continuously sampled through the pinhole and were collimated by a 1.0 mm orifice skimmer mounted at 3.0 mm from the pinhole in the reaction tube. The molecular beam was introduced into the ionization region of the TOFMS, and the molecular species were ionized by the 118 nm photons. The ionized species were accelerated by the electrodes, electronic lenses, and deflectors through the field free drift tube to the multichannel plate (MCP). The MCP passed the information to

8310 *J. Phys. Chem. A, Vol. 111, No. 34, 2007*

Shukla et al.

a digital oscilloscope through an amplifier. Mass spectra were recorded at different temperatures (1136−1507 K) and pressures (8.25−15.11 Torr) with a constant residence time (0.56 s).

Occurrences of a small amount of electron impact ionization resulting from photoelectrons produced by scattered light within the ionization region and of multiphoton ionization that cause fragmentation are ruled out by the absence of any species having an IP greater than 10.5 eV and the absence of any fragment species at room temperature. The reaction tube was cleaned every time before the experiment to avoid contamination from the condensate substances, although tar was only observed outside the heater zone in the downstream.

Results

Explanation of Necessary Basic Terms. For the meaningful interpretation of the mass spectra by solving the complexity, first several sequences of mass numbers of PAHs appearing in the mass spectra are defined here. Note that the designations given here are temporal, only for the discussion in this document.
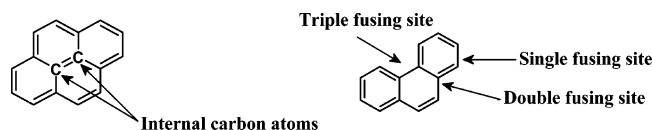
Primary Sequence: Alternate PAHs (Six-Membered Rings PAHs). *Linear-Chain PAHs.* Six-membered ring PAHs having a chain of benzene rings interconnected to each other and lacking internal carbons include
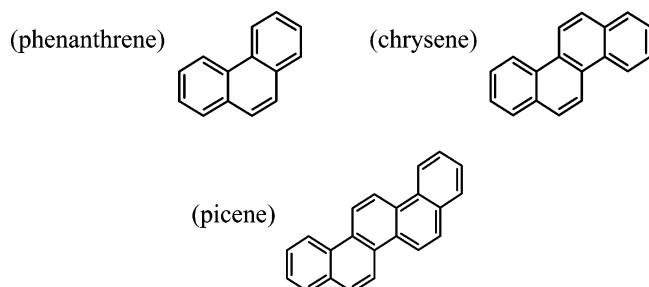
The chemical formulas of such PAHs are

$$C_2H_4 + n(C_4H_2) \quad [a_n]$$
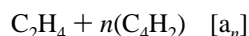
where n is the number of aromatic rings, $n = 1, 2, 3...$, which are hereinafter designated as "a_n".

Condensed PAHs. Six-membered ring PAHs having two or more even-number of internal carbons include
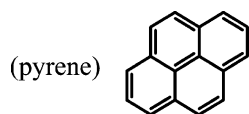
The chemical formulas for such PAHs are

$$C_2H_4 + n(C_4H_2) - m(C_1H_1) \quad [a_n d_m]$$
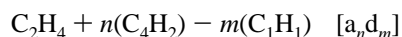
where m is the number of internal carbon atoms, $m = 2, 4, 6...$, which are hereinafter designated as "$a_n d_m$".

Ethynyl or Cyclopenta Acetylene Addition Sequence. PAHs containing one or more ethynyl groups or five-membered rings derived from the primary sequence by acetylene addition at the single or double fusing site, for example,

Their chemical formulas are

$$C_2H_4 + n(C_4H_2) - m(C_1H_1) + l(C_2) \quad [a_n(d_m)C_l]$$
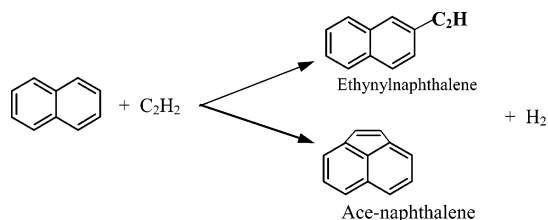
where l is the number of C_2 additions, $l = 1, 2, 3...$, which are hereinafter designated as "$a_n (d_m)C_l$".

Odd Carbon Number Sequence. Methyl-substituted PAHs derived from the primary sequence by the addition of a methyl radical, such as methylphenanthrene

Their chemical formulas are

$$C_2H_4 + n(C_4H_2) - m(C_1H_1) + (C_1H_2) \quad [a_n(d_m)m] \text{ or } [a_n(d_m)\text{-CH}_3]$$
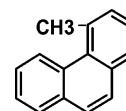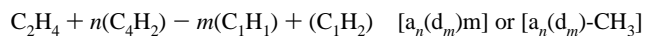
When the attached methyl group forms a new five-membered ring by H_2-elimination and ring closing process, for example,

their formulas become

$$C_2H_4 + n(C_4H_2) - m(C_1H_1) + (C_1) \quad [a_n(d_m)^h C] \text{ or } [a_n(d_m)\text{-}c\text{-CH}_2]$$
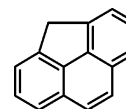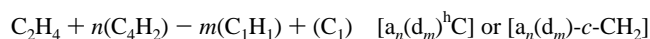
which further changed to a stable radical with a resonance electronic structure such as
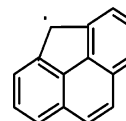
similar to cyclopentadienyl and indenyl; they can be represented by the new formulas

$$C_2H_4 + n(C_4H_2) - m(C_1H_1) + (C_1) - (H_1) \quad [a_n(d_m)\text{-}c\text{-CH}^\bullet]$$
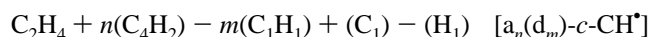
Phenyl Addition Sequence. When PAHs in the primary sequence are attacked by a phenyl radical, they form partly nonfused PAH, such as phenylnaphthalene
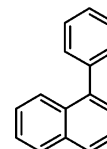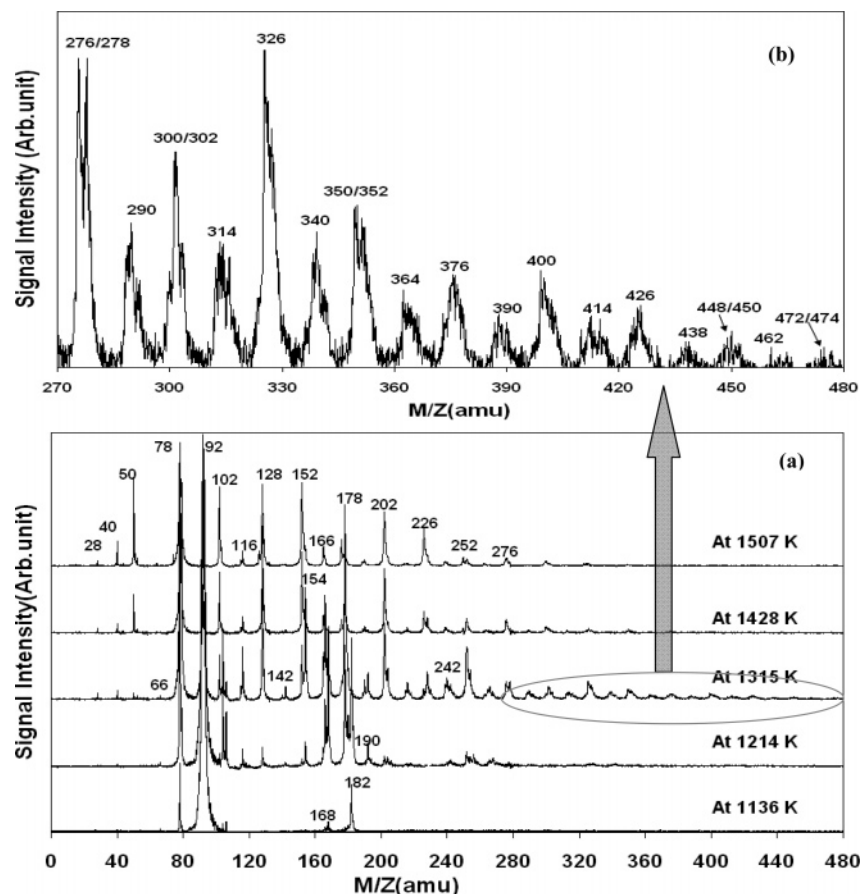
Figure 2. (a) Typical time-of-flight mass spectra of products of toluene pyrolysis at different temperatures and constant pressure 10.12 Torr with constant residence time 0.56 s. (b) Mass spectra of large PAHs at 1315 K (enclosed into an oval shape) at the enlarged scale for clear observation.

and phenylphenanthrene

Their chemical formulas are

$$C_2H_4 + n(C_4H_2) - m(C_1H_1) + (C_6H_4) \quad [a_n(d_m)\text{-}a_1]$$
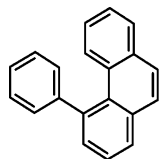
which are, hereinafter, designated as "$a_n(d_m)$-a_1".

Overview on Mass Spectra. Typical TOF mass spectra of products of toluene pyrolysis at various temperatures (1136−1507 K) and constant pressure of 10.12 Torr with constant residence time of 0.56 s are shown in Figure 2. TOF mass spectra of products of pyrolysis of toluene and acetylene mixture under similar experimental conditions are shown in Figure 3. These figures show that toluene thermal decomposition only started above 1100 K under the present experimental conditions. In both cases mass spectral patterns show that the number of peaks increases toward higher masses with increasing temperature up to 1315 K, and above it the number of peaks decreases with increasing temperature. Experimental mass spectra of products of toluene pyrolysis at different total pressures ranging from 8.25 to 15.11 Torr are shown in Figure 4.

The major differences observed from the mass spectra in the case of a toluene and acetylene mixture (Figure 3) over only toluene pyrolysis (Figure 2) are as follows:

(i) appearance of indene ($m/z = 116$ amu) as the major product instead of benzene ($m/z = 78$ amu) and the absence of bibenzyl peak in the low-temperature zone;

(ii) domination of peaks for the species with masses $m/z = 102, 152, 166$, and 178 amu over the species with masses $m/z = 104, 154, 168$, and 182 amu just opposite to the results of only toluene pyrolysis;

(iii) remarkable differences in temperature based signal intensity profiles of the species with masses $m/z = 40, 50, 102, 116, 128, 152, 178, 202$, and 228 amu (shown in Figure 5) are found (the noticeable increase in signal intensities of species in the toluene and acetylene mixture is caused by the direct contribution of the hydrogen abstraction and acetylene addition (HACA) mechanism in the formation of those species due to presence of sufficient acetylene in the mixture);

(iv) suppression of mass signals of phenyl PAHs [$a_n(d_m)$-a_1] and methyl PAHs [$a_n(d_m)$-m or $a_n(d_m)$-CH_3] such as a_1-a_1 (biphenyl, $m/z = 154$ amu) and a_3-CH_3 (methylphenanthrene, $m/z = 192$ amu) after the addition of acetylene.

Comparing both results at different temperatures it is found that at 1136 K significant peaks at $m/z = 78$ amu and $m/z = 182$ amu assigned to benzene (major product) and bibenzyl are observed in the case of toluene pyrolysis. On the other hand significant peaks at $m/z = 116$ amu, $m/z = 78$ amu and $m/z = 40$ amu assigned to indene (major product), benzene, and propyne are observed in the case of the toluene and acetylene mixture. This change in the major product is directly accountable to the HACA mechanism. At 1214 K, new peaks appear together with an increase in intensities of previous peaks in both cases. In only toluene pyrolysis, the main feature is the appearance of a_n species, mainly a_2 (naphthalene, $m/z = 128$) and a_3 (phenan-

8312 *J. Phys. Chem. A, Vol. 111, No. 34, 2007*

Shukla et al.
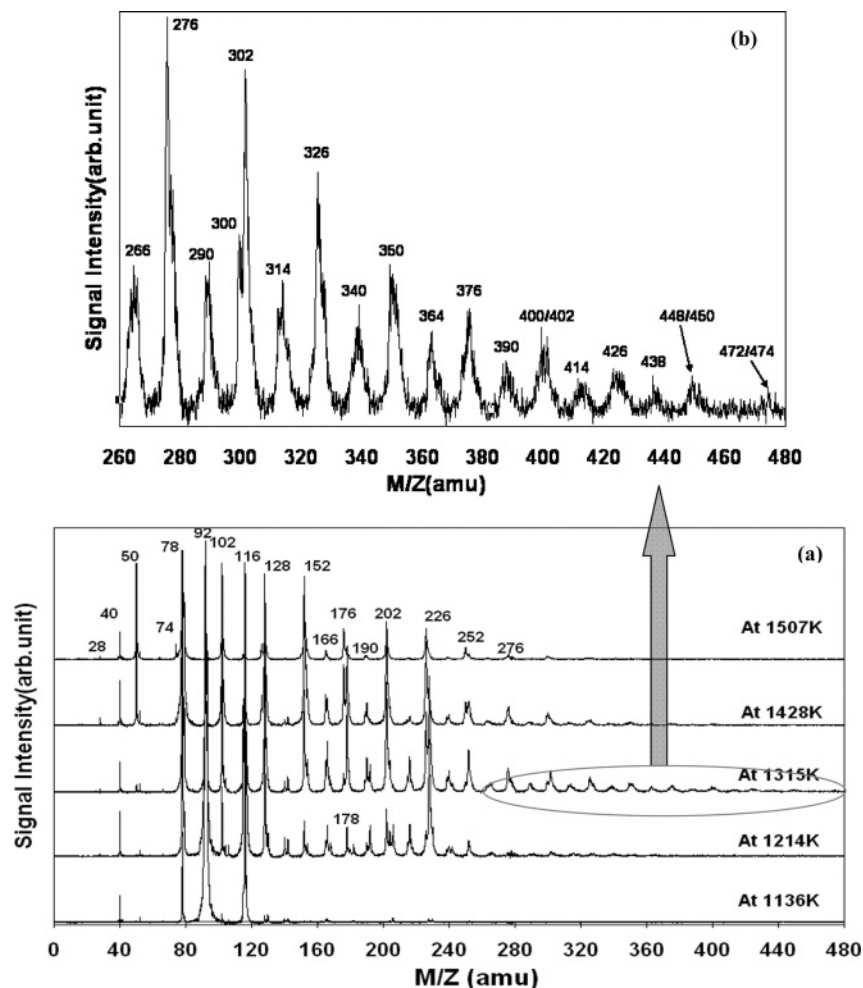
Figure 3. (a) Typical time-of-flight mass spectra of pyrolysis products of the toluene and acetylene mixture at different temperatures and a constant pressure of 10.12 Torr with a constant residence time of 0.56 s. (b) Mass spectra of large PAHs at 1315 K (enclosed into an oval shape) at the enlarged scale for clear observation.

threne, $m/z = 178$), including some peaks out of sequence at $m/z = 104, 106, 116, 154, 166$, and 168 amu. On the other hand many new peaks appear in the case of the toluene and acetylene mixture. Especially some sequences of PAHs and their derivatives are detected. Those products include a_n species a_2, a_3, and a_4 (benzo[c]phenanthrene or chrysene, $m/z = 228$), $a_n d_m$ species $a_4 d_2$ (pyrene, $m/z = 202$) and $a_5 d_2$ (benzo[e]pyrene, $m/z = 252$), $a_n(d_m)C_l$ species $a_1 C_1$ (phenylacetylene, $m/z = 102$) and $a_2 C_1$ (acenaphthalene, $m/z = 152$) together with $a_n(d_m)$-CH$_3$ species a_2-CH$_3$ (methylnaphthalene, $m/z = 142$), a_3-CH$_3$ (methylphenanthrene, $m/z = 192$), $a_4 d_2$-CH$_3$ (methylpyrene, $m/z = 216$), and a_4-CH$_3$ (methylbenzo[c]phenanthrene or methylchrysene, $m/z = 242$). These observed products clearly show that products in only toluene result from a combination of radicals produced mainly from toluene and benzyl decompositions. On the other hand almost all products in the case of the toluene and acetylene mixture result from the trapping of resulting radicals by acetylene present in the mixture except some a_n species such as a_4, produced by radical−radical addition, and $a_n(d_m)$-CH$_3$ species, produced by methyl radical attack on the respective neutral species.

At 1315 K, the maximum product species of different varities ranging from methyl radical to large PAHs up to mass 474 amu are detected. Many sequences of product species are observed. Those sequences include linear chain PAHs (a_n), condensed PAHs ($a_n d_m$), phenyl PAHs [$a_n(d_m)$-a_1], methyl-substituted PAHs [$a_n(d_m)$-CH$_3$], and cyclopenta-fused PAHs [$a_n(d_m)$-c-CH$_2$] in the case of toluene (Figure 9) while the disappearance of methyl

PAHs [$a_n(d_m)$-CH$_3$] and phenyl PAHs [$a_n(d_m)$-a_1] together with the appearance of ethynyl derivatives of PAHs [$a_n(d_m)$-C_1] are detected as two unique differences in the case of the toluene and acetylene mixture (Figure 10). This change of product species well explains the trapping of methyl, phenyl, and PAHs radicals by acetylene to result in propyne, phenylacetylene, and ethynyl derivatives of PAHs.

At 1428 K the large PAHs signals begin to disappear along with a decrease in signal intensities of lower PAHs. At the mean time signals of some new smaller species such as propyne ($m/z = 40$) and diacetylene ($m/z = 50$) appeared in the case of only toluene, while only diacetylene appeared in the case of toluene and acetylene mixture. At 1507 K, the disappearance of PAHs of higher masses and phenyl PAHs [$a_n(d_m)$-a_1] are observed. On the other hand new peaks for polyynes ($C_{2n}H_2$), ethynyl [$a_n(d_m)$-C_1], and diethynyl [$a_n(d_m)$-C_2] derivatives of PAHs are detected in the case of only toluene pyrolysis (Figure 11), while no remarkable differences are observed in the case of the toluene and acetylene mixture (Figure 12).

Pressure-dependent mass spectra (Figure 4) were taken at a constant temperature of 1315 K and a constant residence time of 0.56 s. Observed mass spectra show that an increase in pressure increases the number of species toward the higher mass region with an increase in the intensities. The effect of pressure is confirmed by the observation of clear signals of large PAHs at masses $m/z = 448$ amu ($C_{36}H_{16}$) and $m/z = 472$ amu ($C_{38}H_{16}$) with weak peaks (trace amounts) at masses $m/z = 496$ amu ($C_{40}H_{16}$), $m/z = 520$ amu ($C_{42}H_{16}$), and $m/z = 522$ amu ($C_{42}H_{18}$)

PAH Formation in Toluene Pyrolysis

J. Phys. Chem. A, Vol. 111, No. 34, 2007 **8313**
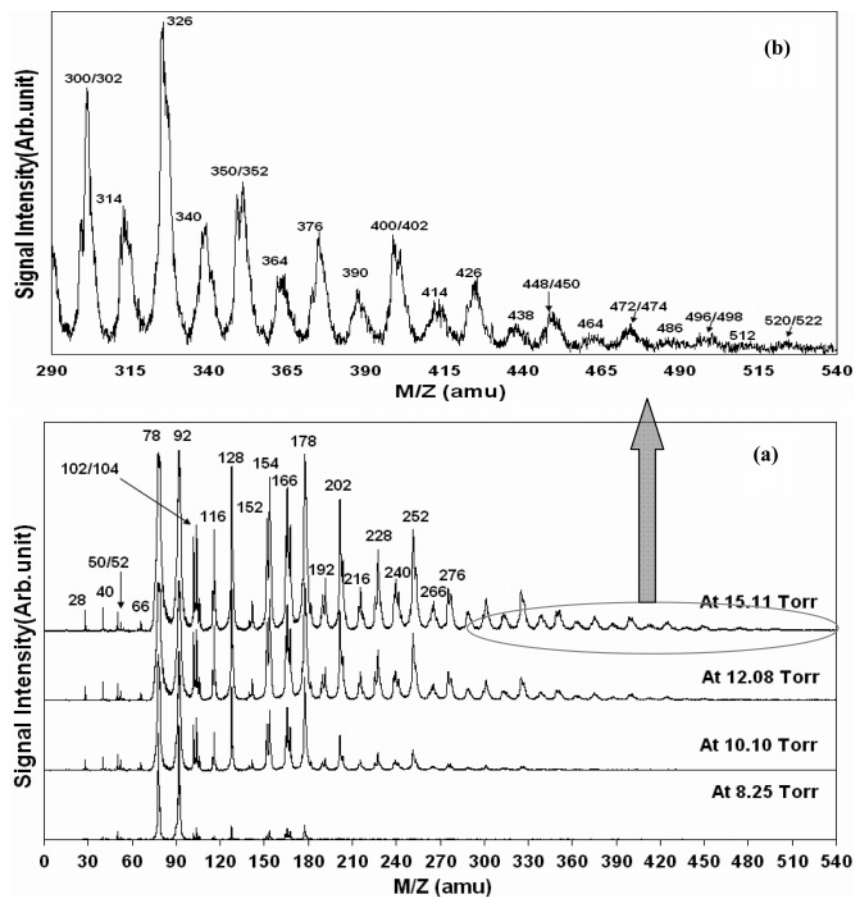
Figure 4. (a) Experimental mass spectra of products of toluene pyrolysis at different pressures (8.25−15.11 Torr) and a constant temperature of 1315 K with a constant residence time of 0.56 s (b) Mass spectra of large PAHs at 15.11 Torr (enclosed into an oval shape) at the enlarged scale for clear observation.

at a pressure of 15.11 Torr. These species are not observed in temperature-dependent mass spectra taken at 10.12 Torr. Observation of these new species indicates that unimolecular decompositions of toluene and benzyl radical are influenced by the total pressure. A total of 75 species including smaller species, radicals, polyynes, ethynyl, methyl, and phenyl derivatives of PAHs and large PAHs up to mass $m/z = 522$ amu ($C_{42}H_{18}$) are identified in mass spectra (Figures 2−4). The detected species are listed in Table 1 with their masses and chemical formulas. Taking into account the complexity of the isomers especially above a_3 and explanation 1 just below, names and notations are not assigned for the species listed in the Table 1. Detailed analysis of mass spectra at 1315 K is presented in Figure 9 for only toluene and in Figure 10 for the toluene and acetylene mixture. Similarly, mass spectra at 1507 K are presented in Figure 11 for only toluene and in Figure 12 for the toluene and acetylene mixture. In these figures some points should be noted for clear discussion, such as:

1. In each series, symbols with the mass numbers specific to the series, i.e., the mass numbers that uniquely belong to the series and do not overlap with the mass numbers in other series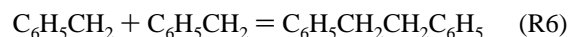, are indicated over the horizontal line of the series with larger letters, while those that are not unique to the series are indicated below the horizontal line with smaller letters. Also, symbols were not even shown for some overlapping mass numbers to avoid complexity.

2. For compounds with the c-CH_2 group, that is, indene, fluorene, and the $a_n(d_m)^h c$ series, the mass numbers belonging

to the resonantly stabilized radicals such as indenyl
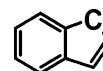
are indicated by the dotted lines starting from the parent molecules.

Discussion

Although the pyrolysis of toluene has been a subject of discussion for a long time[23] the information regarding the gas-phase products is extremely limited. Szwarc et al.[24] proposed only bibenzyl as the product, and further the number of products increased in other studies,[10,30−31,34,38,57] but still it is limited only up to benzo[a]pyrene, $C_{20}H_{12}$. Present experimental results agree with the results obtained by Smith et al.[30,31] He pointed out that radical species play a more important role in the formation of PAHs in aromatic pyrolysis. Smith et al. reported the production of PAH species up to $C_{20}H_{12}$ and traces of $C_{24}H_{12}$ at temperatures of 1673−2173 K and low pressures. In the present study, PAH species up to mass $m/z = 474$ amu ($C_{38}H_{18}$) and traces of $m/z = 496$ amu ($C_{40}H_{16}$), $m/z = 498$ amu ($C_{40}H_{18}$), $m/z = 520$ amu ($C_{42}H_{16}$), and $m/z = 522$ amu ($C_{42}H_{18}$) have been detected. For the discussion of the chemical kinetic mechanism for the formation of observed products, three temperature regions can be distinguished on the basis of mass pattern in Figures 2 and 3: (i) In the low-temperature region (<1300 K), mainly a_n species from benzene to phenanthrene (a_3) are observed, and their formation is dominated by radical−
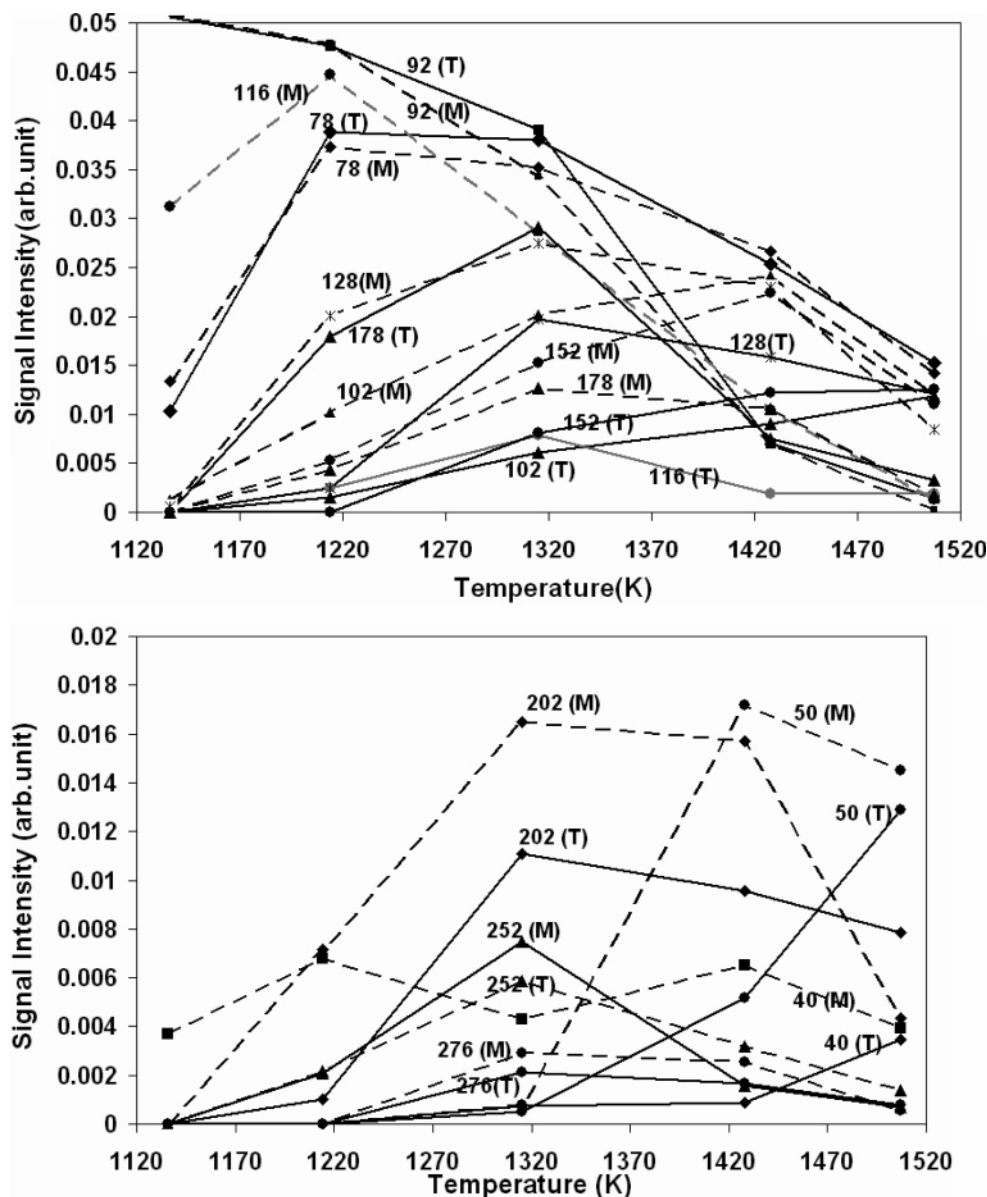
Figure 5. Temperature-dependent variation of signal intensities of products of both toluene and the toluene + acetylene mixture. The solid line represents results from toluene, and the dotted line represents results from the toluene and acetylene mixture. Numbers represent the masses of the species. Inside the bracket T stands for the species from toluene, and M stands for the species from the toluene and acetylene mixture.

radical and radical-molecule reactions. (ii) In the moderate temperature region (from 1300 to 1428 K), the formation of large PAHs up to $m/z = 474$ amu including their methyl and phenyl derivatives and cyclopenta-fused PAHs are remarkable. Formation of those products is dominated by the radical−radical reactions with major role of cyclopenta-fused radicals such as cyclopentadienyl and indenyl radicals and radical-molecule reactions with major role of phenyl attack on PAHs. Growth of large PAHs also involves the active role of the HACA (hydrogen abstraction and acetylene addition) mechanism for ring growth in one step. (iii) In the high-temperature region (>1500 K), the disappearance of higher mass species (large PAHs) and appearance of some new species of relatively smaller masses are of particular interest. Newly observed species mainly include small species, polyynes, and diethynyl derivatives of PAHs. The formation of these species in this temperature region is dominated by the HACA.

Chemical Kinetics in the Low-Temperature (<1300 K) Region. For an overview, see Figure 6, which contains a comparison of mass spectra only at low temperatures.

At 1136 K, a change in the major product from benzene to indene and a disappearance of bibenzyl in the case of the toluene and acetylene mixture together with absence of biphenyl in both cases are remarkable.

At 1214 K, a significant difference in signal intensities of linear PAHs mainly a_2 and a_3 and an appearance of a_4 only in the toluene and acetylene mixture are noticeable. This corresponds to the formation of these species by different reaction routes. Another unique feature is the appearance of lower members of condensed PAHs ($a_n d_m$), methyl-substituted small PAHs [$a_n(d_m)$-CH$_3$], and ethynyl derivatives of small PAHs [$a_n(d_m)C_1$] in the case of the toluene and acetylene mixture.

Detailed Interpretations and Expected Mechanisms. The significant signal at $m/z = 182$, most probably bibenzyl, is

PAH Formation in Toluene Pyrolysis

J. Phys. Chem. A, Vol. 111, No. 34, 2007 **8315**
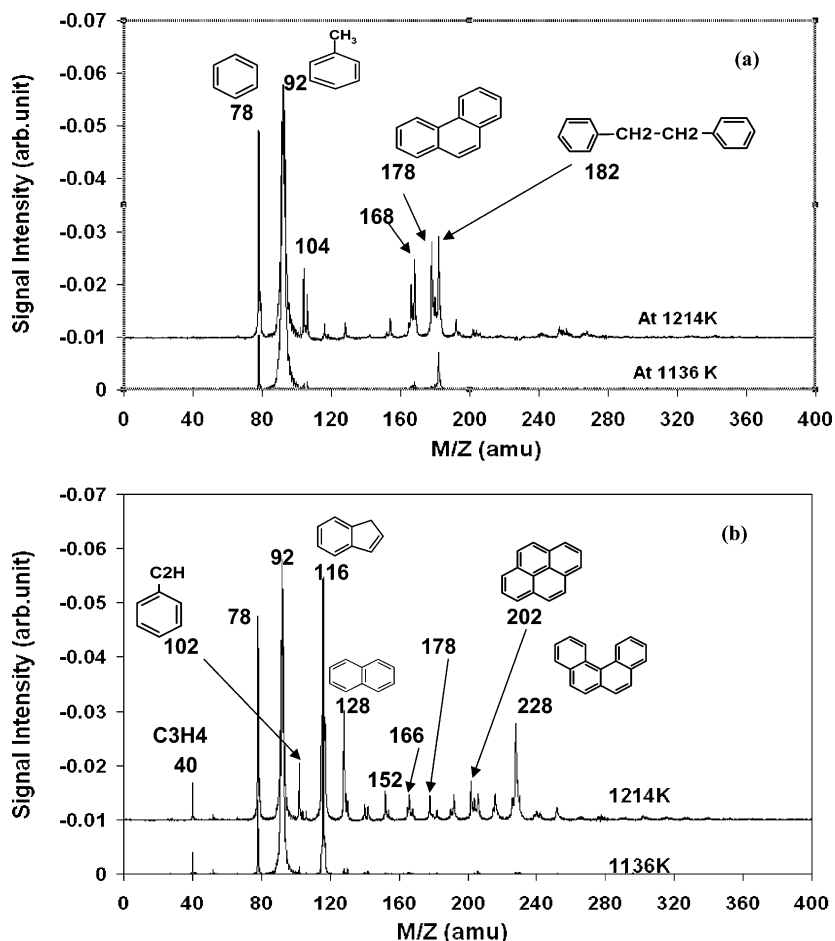
Figure 6. (a) Experimental mass spectra of products of toluene pyrolysis at a temperatures of 1136 and 1214 K. (b) Mass spectra of products of toluene + acetylene pyrolysis for comparison of results.

produced by the recombination of benzyl radicals in the case of only toluene. In the case of the toluene and acetylene mixture the major product's signal at $m/z = 116$, assigned to indene, resulted from the trapping of the benzyl radical by acetylene (R12). Such phenomena of trapping of a radical are also supported by the appearance of propyne ($m/z = 40$) produced due to the trapping of a methyl radical by acetylene in the case of the toluene and acetylene mixture. Absence of biphenyl in both cases is evidence for the production of the benzyl radical in a rather higher concentration than phenyl at 1136 K. These results agree with previous studies[10,21,25−27,29,44,58,59] for the domination of decomposition of toluene through reaction R1 over R2

$$C_6H_5CH_3 + M = C_6H_5CH_2 + H + M \quad (R1)$$

$$C_6H_5CH_3 + M = C_6H_5 + CH_3 + M \quad (R2)$$
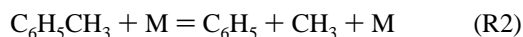
Smith et al.[30,31] reported the same conclusion based on the observation of the mass spectrum of hydrogen at 1000 °C. The same result is also obtained by the recent studies of Klippenstein et al.[50] and Oehlschlaeger et al.[60] based on the estimation of rate constants with the activation energy barrier for R1 ($E_a = 87.51$ kcal) and for R2 ($E_a = 97.88$ kcal). The branching ratio, $k_1/(k_1 + k_2)$, estimated by them is 0.8 at 1350 K. According to these studies, the branching ratio is inversely proportional to the temperature and pressure. It means that at the low-temperature and low-pressure region (1136 K and 10.12 Torr) at which toluene decomposition started in this study the branching ratio should be very high. This results in a higher

concentration of benzyl radical than phenyl radical. The higher concentration of benzyl radical also might be due to its formation through reactions R3−R5 while phenyl radical formation through similar types of reactions (i.e., methyl abstraction by radicals) is difficult due to very slow rates.[27] At the same time benzyl radical recombines to form bibenzyl (R6) and phenyl radical recombines to form biphenyl (R7)

$$C_6H_5CH_3 + H = C_6H_5CH_2 + H_2 \quad (R3)$$

$$C_6H_5CH_3 + CH_3 = C_6H_5CH_2 + CH_4 \quad (R4)$$

$$C_6H_5 + C_6H_5CH_3 = C_6H_5CH_2 + C_6H_6 \quad (R5)$$

$$C_6H_5CH_2 + C_6H_5CH_2 = C_6H_5CH_2CH_2C_6H_5 \quad (R6)$$

$$C_6H_5 + C_6H_5 + M = C_6H_5 C_6H_5 + M \quad (R7)$$
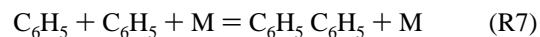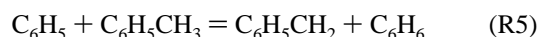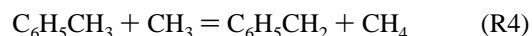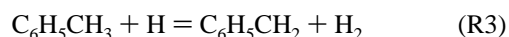
Muller-Markgraf et al.[61] and Brouwer et al.[27] have reported almost equal rate constants for both recombination reactions (R6 and R7) without any energy barriers. Both phenyl and benzyl radicals are also consumed by the radical combination reactions R8 and R9 for the formation of benzene and ethylbenzene

$$C_6H_5 + H + M = C_6H_6 + M \quad (R8)$$

$$C_6H_5CH_2 + CH_3 = C_6H_5CH_2CH_3 \quad (R9)$$
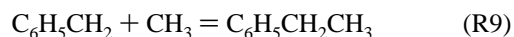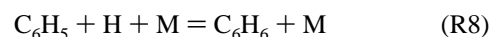
Further consumption of biphenyl into a_3 is not possible due to the absence of C_2H_2 in the mixture while the conversion rate of bibenzyl into stilbene is expected to be much slower than its
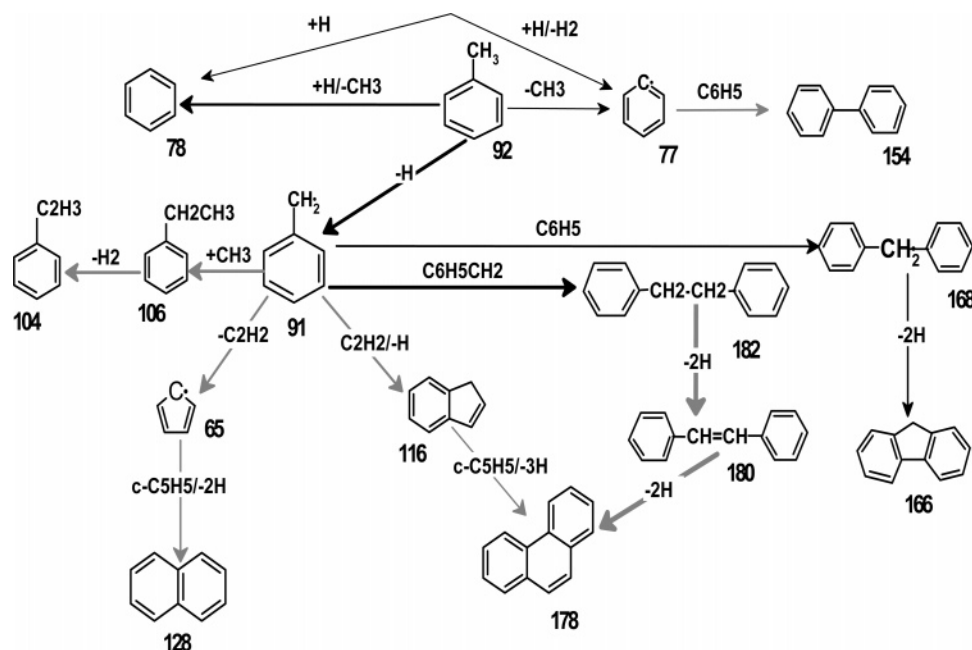
Figure 7. Formation mechanism of products of toluene pyrolysis at 1136 and 1214 K showing clearly the domination of radical−radical and radical−molecule reactions. Black arrows indicate reaction routes at 1136 K, and gray arrows indicate reaction routes at 1214 K. Thick arrows indicate dominant routes, and numbers represent molecular masses.

rate of formation due to a high activation energy barrier[27] (E_a for R6 = 0.5 kcal while E_a for R15 = 51.9 kcal). The above discussion suggests that the concentration of bibenzyl should be higher than that of biphenyl. The observation of bibenzyl and the absence of biphenyl in the present study also well agrees with this expectation. The biphenyl peak could not be observed at this temperature because of a low concentration of phenyl radical as phenyl radical is also consumed to form benzylbenzene by reaction R10

$$C_6H_5CH_2 + C_6H_5 = C_6H_5CH_2C_6H_5 \qquad (R10)$$
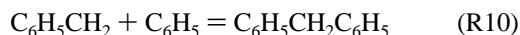
This is confirmed by the presence of a weak peak of benzylbenzene. Observation of benzene as a major product favors its formation through reactions R8 and R11 and no further consumption or decomposition at this temperature

$$C_6H_5CH_3 + H = C_6H_6 + CH_3 \qquad (R11)$$

$$C_6H_5CH_2 + C_2H_2 = C_9H_8 + H \qquad (R12)$$
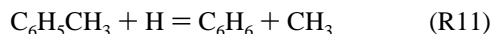
The observation of indene as the major product instead of benzene in the case of the toluene and acetylene mixture is due to lack of its consumption or decomposition while benzene is consumed for the formation of phenylacetylene through the HACA mechanism, which is supported by the weak peak of phenylacetylene in the beginning of decomposition process and a significant peak at higher temperatures.

At 1214 K, the appearance of new peaks for indene and a_2 (naphthalene) in the case of only toluene indicates the initiation of the decomposition of the benzyl radical through reaction R13 as these species involve acetylene and the cyclopentadienyl radical in their formation

$$C_6H_5CH_2 + M = c\text{-}C_5H_5 + C_2H_2 + M \qquad (R13)$$
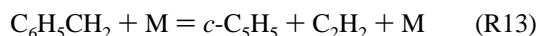
Similar results are reported by Shivaramakrishnan et al.[49] The variation in the concentration of a_n species can be explained by the difference in their formation routes and further consumptions. The weak signal of a_2 in the case of only toluene suggests

only contribution of reaction R14 with a low concentration of $c\text{-}C_5H_5$ while in the case of the toluene and acetylene mixture, a_2 is found to be produced by the major contribution of two different reactions, first by the HACA reaction from phenylacetylene and next by reaction R15 from the addition of benzyl and propargyl radicals, as both radicals are resonantly stablized. The HACA route is backed up by the appearance of the significant signal of phenylacetylene, and reaction R15 is supported by the appearance of propyne from 1136 K, which can easily form the propargyl radical by reaction R16. But the minor contribution of reaction R14 also cannot be ignored as benzyl decomposition has already started at this temperature. The contribution of reactions R15 and R16 and the HACA for the formation of a_2 above 1315 K in the case of only toluene is also significant based on the appearance of propyne and phenylacetylene. Formation of a_2 by reaction R14 is also proposed by D'Anna et al.[62,63] and Skjoth-Rasmussen et al.[9] as the controlling path for aromatic ring growth. Similarly, formation of a_2 by reaction R15 is first proposed by Colket et al.[79] and further supported by McEnally et al.[80,81] based on their experimental study on methane/air non-premixed flames doped with toluene and ethylbenzene

$$c\text{-}C_5H_5 + c\text{-}C_5H_5 = a_2 + 2H \qquad (R14)$$

$$C_6H_5CH_2 + C_3H_3 = a_2 + 2H \qquad (R15)$$

$$C_3H_4 + H = C_3H_3 + H_2 \qquad (R16)$$
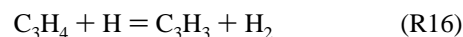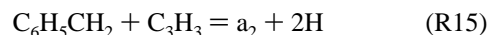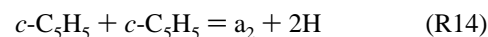
The appearance of a weak signal for a_3 (phenanthrene) and the absence of a biphenyl signal in the case of the toluene and acetylene mixture support the formation of a_3 from biphenyl (m/z = 154 amu) by the HACA mechanism.[64] Similarly, the observation of a_4d_2 (pyrene, m/z = 202) and a_5d_2 (benzo[e]pyrene, m/z = 252) also support the further consumption of a_3 to form pyrene by the HACA and benzo[e]pyrene by phenyl attack. But a significant peak of a_3 and a weak signal of stilbene (m/z = 180) in only toluene pyrolysis suggest different routes from the HACA due to very low concentrations of both biphenyl
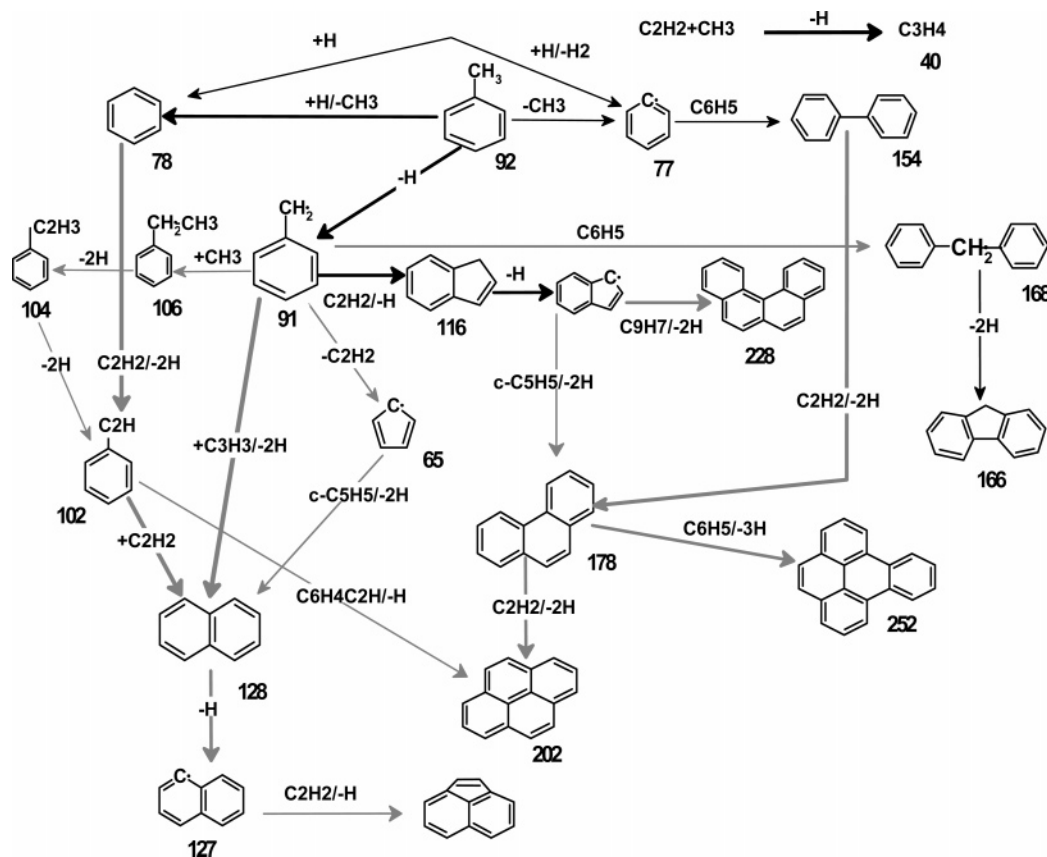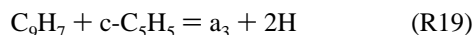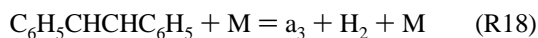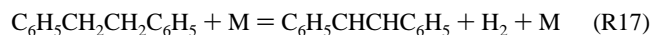
PAH Formation in Toluene Pyrolysis

*J. Phys. Chem. A, Vol. 111, No. 34, 2007* **8317**

Figure 8. Formation mechanism of products of toluene + acetylene pyrolysis at 1136 and 1214 K showing clearly the influence of the HACA mechanism together with aromatic radical−radical and radical−molecule reactions. Black arrows indicate the reaction routes at 1136 K, and gray arrows indicate reaction routes at 1214 K. Thick arrows indicate dominant routes, and numbers represent molecular masses.

and acetylene. They favor the consecutive reactions R17 conversion of bibenzyl into stilbene by H_2 elimination and reaction R18 conversion of stilbene into a_3 by H_2 elimination and ring closing reactions as dominant routes. Reaction R19 also can contribute significantly in the formation of a_3 due to a low-energy process, but the concentration of c-C_5H_5 is expected to be low at this temperature in both cases

$$C_6H_5CH_2CH_2C_6H_5 + M = C_6H_5CHCHC_6H_5 + H_2 + M \quad (R17)$$

$$C_6H_5CHCHC_6H_5 + M = a_3 + H_2 + M \quad (R18)$$

$$C_9H_7 + c\text{-}C_5H_5 = a_3 + 2H \quad (R19)$$

Bruinsma et al.[65] and Errede et al.[57] have well demonstrated the conversion paths of bibenzyl into stilbene and phenanthrene (a_3). The observation of a significant peak at $m/z = 228$ only in the case of the toluene and acetylene mixture is assigned to a_4 (Benzo[c]phenanthrene or chrysene). The increase in the signal intensity of a_4 and the sharp fall in the intensity of indene above 1214 K indicate its formation by the recombination of indenyl radicals[83] by reaction R20

$$C_9H_7 + C_9H_7 = C_{18}H_{12} (a_4) + H_2 \quad (R20)$$
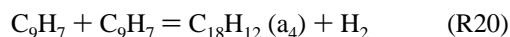
It seems reasonable to explain the observation of methyl PAHs [$a_n(d_m)$-CH_3] and ethynyl PAHs [$a_n (d_m)$-C_1] only in the case of the toluene and acetylene mixture because of the direct attack of the methyl radical on the corresponding a_n or $a_n(d_m)$ species and the trapping of PAH radicals by C_2H_2 present in the mixture.

Their formation routes are explained in detail in the next section (moderate temperature region). Kinetic discussion of this temperature region can be concluded as: (a) Toluene decomposition into the benzyl radical and hydrogen is dominant. (b) Reaction mechanisms below 1300 K are dominated by radical−radical and radical−molecule reactions in the case of only toluene while there is also an effect of HACA in the case of the toluene and acetylene mixture. (c) Formation routes of a_2 (naphthalene) and the first member of PAH a_3 (phenanthrene) in toluene pyrolysis with and without addition of acetylene are completely different. The detailed overviews of the above-discussed reaction flow paths are summarized in Figure 7 and Figure 8.

Chemical Kinetics in the Moderate Temperature (1300−1428 K) Region. At 1315 K, the appearance of many new signals from lower to higher masses (15−474 amu) and the disappearance of the bibenzyl signal in the case of only toluene and a sharp fall in the intensity of indene in the case of the toluene and acetylene mixture are in good agreement with the observations of Hippler et al.[29] and Jones et al.[67] They indicated that the rate of recombination of benzyl radicals and its reaction with other aromatic species significantly reduced while the rate of decomposition of the benzyl radical significantly increased above 1300 K. The disappearance of bibenzyl and stilbene signals, a rather weak signal for indene, and the dominant peak of a_3 (greater than all PAHs) are expected to result from the acceleration of reactions R17−R19. The disappearance of bibenzyl may also be due to its decomposition into the benzyl radical by the reaction R21 followed by decomposition of benzyl

radical through reaction R13 and also trapping of benzyl radical by C_2H_2 to form indene (reaction R12)

$$C_6H_5CH_2CH_2C_6H_5 + M = 2 C_6H_5CH_2 + M \quad (R21)$$
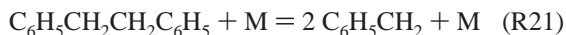
Finally, the dominant routes for the formation of large PAHs through reactions R12, R13, R14, and R19 are accelerated. At this temperature a maximum number of species could be observed in the present study. An overview of Figures 9 and 10 gives the following information:

1. In the pyrolysis of the toluene and acetylene mixture, the observed mass spectra (Figure 10) show regular and monotonic decreases of intensity toward higher mass numbers above ~250 amu while in the only toluene pyrolysis (Figure 9) some noticeable irregularity is found.

2. In the only toluene pyrolysis at 1315 K, where the largest PAHs were observed, the compounds with an odd number carbon atoms seem relatively abundant. When the temperature was raised to 1428 K and above or acetylene was added, their relative intensities became weaker, and the growth of PAHs seems depressed. This implies the role of intermediates with odd carbons, i.e., cyclopentadienyl and cyclopenta-fused aromatic radicals such as indenyl and 4H-cyclopenta[*def*]phenanthrenyl radicals, in the growth of PAHs.

3. Each peak of the primary alternate PAHs is found associated with a +2 mass peak.

Detailed Interpretations and Expected Mechanisms. Weak mass peaks of a_n species above ~a_4 indicate their formation in an inefficient way. Their structure reflects that their formation is only possible by the two-step HACA mechanism, which is expected to be inefficient for faster ring growth. Against this expectation, the observation of significant mass peaks for a_3 and a_4 in the present study can be explained in terms of different reaction routes for their formation as explained previously.

The next abundant PAH is assigned to the first member of the condensed PAH [$a_n d_m$] species, i.e., $a_4 d_2$ ($m/z = 202$) exclusively pyrene, which is easily formed from the acetylene addition to phenanthrene while in the case of the toluene and acetylene mixture self-reaction of phenylacetylene also cannot be ignored, which is supported by the high concentration of phenylacetylene and rather significant signal of pyrene. Other strong peaks continue on higher masses with a C_6 interval, say, $m/z = 252/276, 326/350, ...$, are assigned to $a_5 d_2/a_6 d_4$, $a_7 d_4/a_8 d_6...$ The mechanism relevant to this continuation is implied to be the phenyl radical addition to small PAHs. This is further backed up by the abundance of [$a_n(d_m)$-a_1] peaks, which appear at +2 mass number larger than primary PAHs.

On the basis of abundance of phenyl PAHs [$a_n(d_m)$-a_1] it is not difficult to assume that these species are produced by the reaction of benzene and PAH radicals, phenyl radical, and neutral PAHs or by the direct addition of phenyl and PAH radicals. This is supported by the decrease in signal intensity of benzene above 1214 K. These +2 mass peaks [$a_n(d_m)$-a_1] become weaker at high temperature in the case of only toluene and when acetylene was added at this temperature. This is clearly supported by the significant signal of biphenyl ($m/z = 154$) over acenaphthalene ($m/z = 152$) (Figure 9), which becomes reverse at high temperatures (Figure 11) and after addition of acetylene (Figure 10). This decrease in intensity is expected to be due to trapping of phenyl and PAH radicals before attacking each other by acetylene to form phenylacetylene and ethynyl derivatives of PAHs. This is supported by the appearance of a significant signal of phenylacetylene only at high temperature in the case of only toluene and from the beginning of the decomposition process (1136 K) in the case of the toluene and acetylene mixture.

A decrease in the intensities of phenyl PAHs at high temperatures also might be due to their conversion into new PAHs. Phenyl PAHs produced by the phenyl radical attack at the triple fusing site are changed to condensed (benzenoid) PAHs while phenyl PAHs produced by the phenyl radical attack at the double fusing site are changed to PAHs having a cyclopenta ring enclosed among the six-membered rings (non-benzenoid PAHs) followed by H_2 elimination and ring closing processes. For example, phenylphenanthrene resulted due to the attack of phenyl radical at the triple fusing site of phenanthrene is changed to benzo[*e*]pyrene ($a_5 d_2$), and phenylnapthalene resulted from phenyl radical attack on the double fusing site is changed to fluoranthene ($m/z = 202$), an isomer of pyrene (as shown below in schemes a and b). As resulting products in both cases consist triple fusing sites, they can easily further grow into the large PAHs (either benzenoid or non-benzenoid) both by the HACA mechanism as well as by the phenyl radical attack.


(a)

(b)
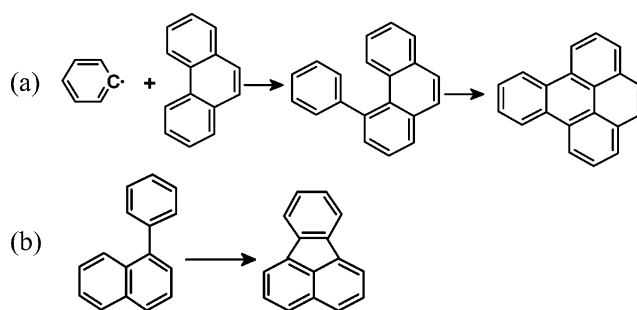
This reaction sequence is also supported by Frenklach et al.[64] who have demonstrated the formation of benzocoronene from the reaction of benzo[*ghi*]perylene and benzene.

The odd carbon number compounds that are prominent in the toluene spectrum at 1315 K are ascribed to be the methyl-substituted PAHs [$a_n(d_m)$-CH_3] and the derived PAHs with a five-membered ring [$a_n(d_m)$-c-CH_2]. At elevated temperatures $a_n(d_m)c$-CH_2 species are dominant over $a_n(d_m)$-CH_3 species. At this temperature, the odd carbon number compounds are accompanied by corresponding radicals [$a_n(d_m)c$-$CH^•$]. From these observations, it is not difficult to assume that methyl-substituted PAHs analogous to toluene are unstable at high temperatures and are converted to corresponding radicals [$a_n(d_m)$-$CH_2^•$] both by direct dissociation and by the attack of free H atoms. These resulting radicals are changed to stable PAHs having a five-membered ring [$a_n(d_m)$-c-CH_2] by H elimination and ring closing reactions. PAHs with a five-membered ring such as 4H-cyclopenta[*def*]phenanthrene
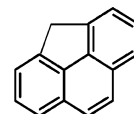
produced from methylphenanthrene
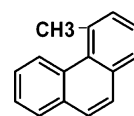
are fairly stable, and their derived radicals

PAH Formation in Toluene Pyrolysis

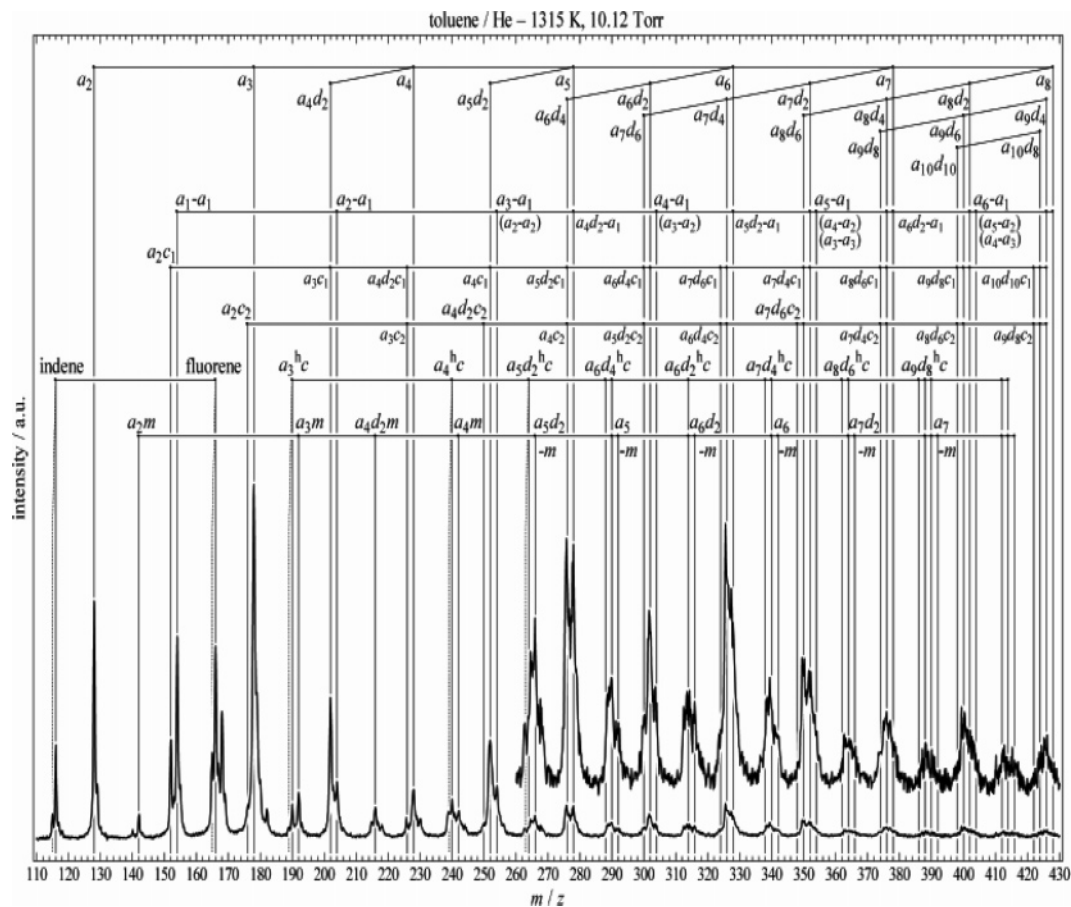*J. Phys. Chem. A, Vol. 111, No. 34, 2007* **8319**

Figure 9. Experimental mass spectra of products ($m/z > 110$) of toluene pyrolysis at a temperature of 1315 K with microanalysis of mass peaks showing many sequences of species.
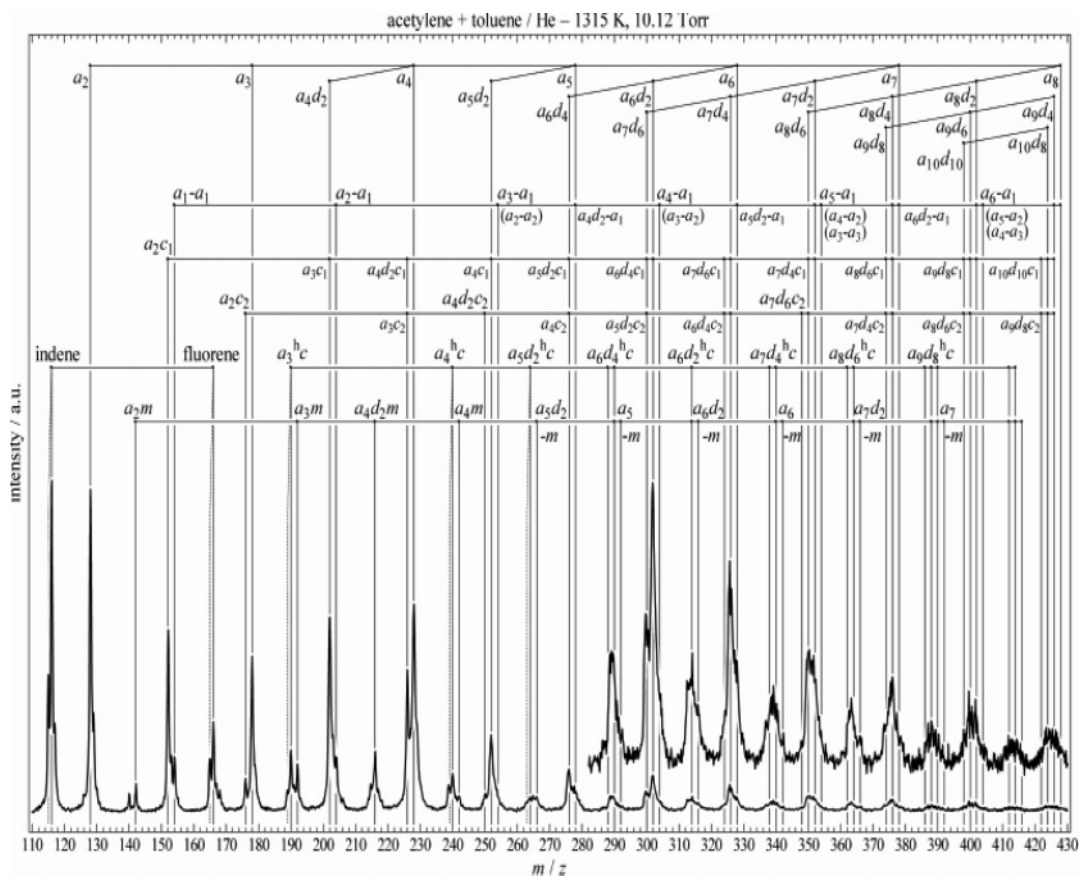

Figure 10. Experimental mass spectra of products ($m/z > 110$) of pyrolysis of the toluene and acetylene mixture at a temperature of 1315 K with microanalysis of mass peaks showing many sequences of species.
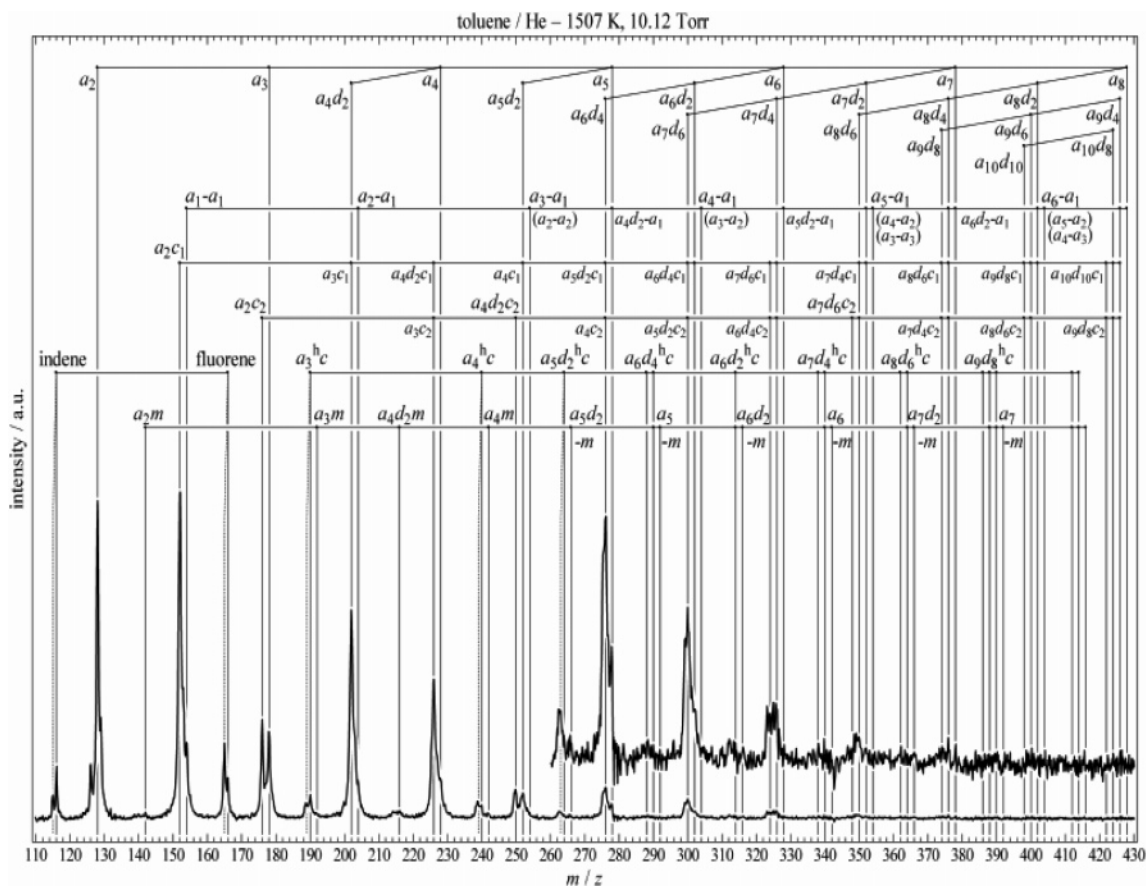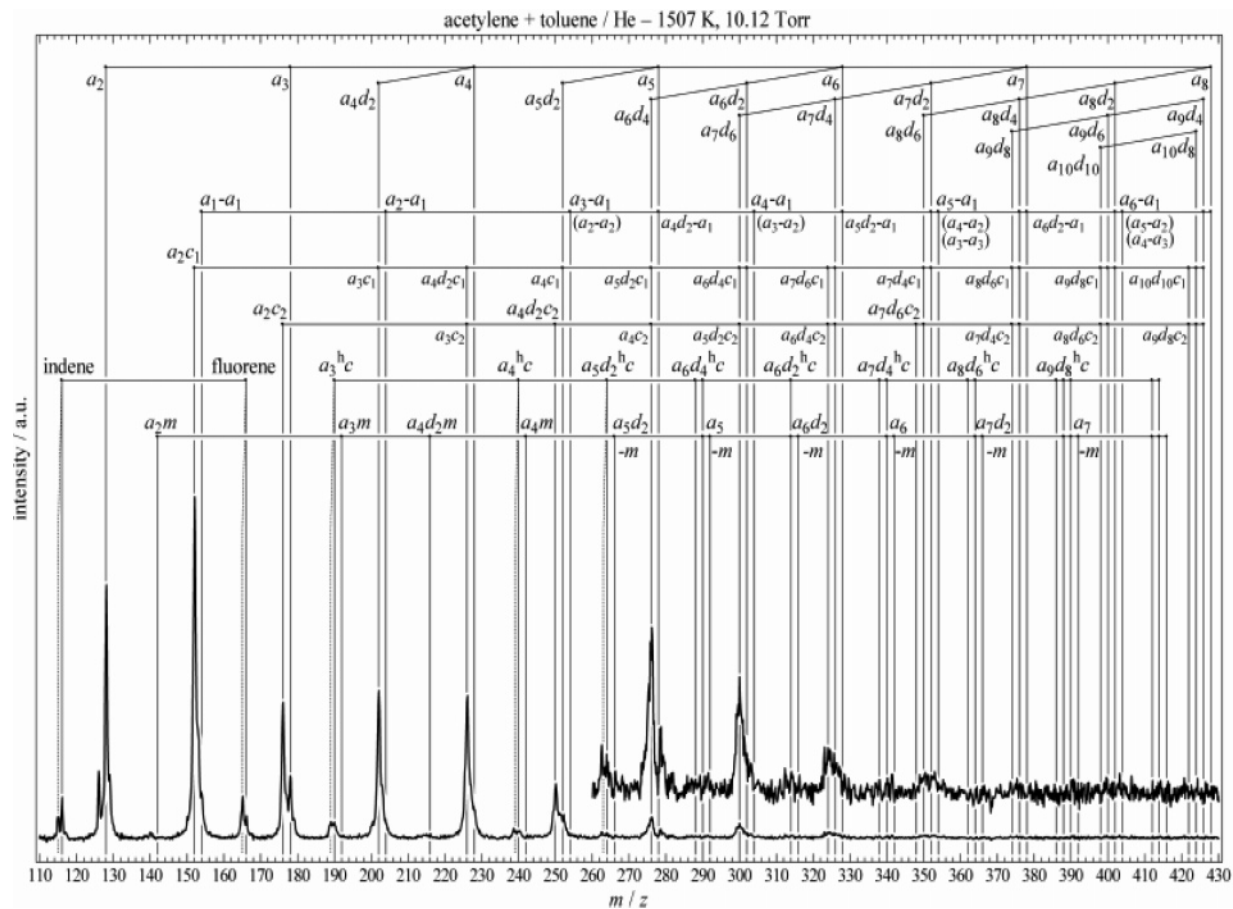
Figure 11. Experimental mass spectra of products ($m/z > 110$) of toluene pyrolysis at a temperature of 1507 K with microanalysis of mass peaks showing many sequences of species.

Figure 12. Experimental mass spectra of products ($m/z > 110$) of pyrolysis of the toluene and acetylene mixture at a temperature of 1507 K with microanalysis of mass peaks showing many sequences of species.

PAH Formation in Toluene Pyrolysis

J. Phys. Chem. A, Vol. 111, No. 34, 2007 **8321**
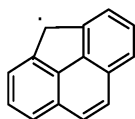
are expected to be very stable with resonance electronic structures similar to cyclopentadienyl

and indenyl
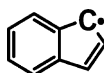
It should be noted that the mass peaks for PAH species with a five-membered ring [$a_n(d_m)$-c-CH_2 or $a_n(d_m)^hC$] are accompanied by the mass peaks with -1 mass, assigned to the resonantly stabilized radicals. This is also clearly supported by the appearance of the mass peaks at $m/z = 115$ amu for indenyl and $m/z = 165$ amu for fluoryl radicals. These resulting radicals are expected to contribute efficiently in the ring growth by the inter- and intramolecular reactions followed by H_2 elimination and ring-closing processes similar to
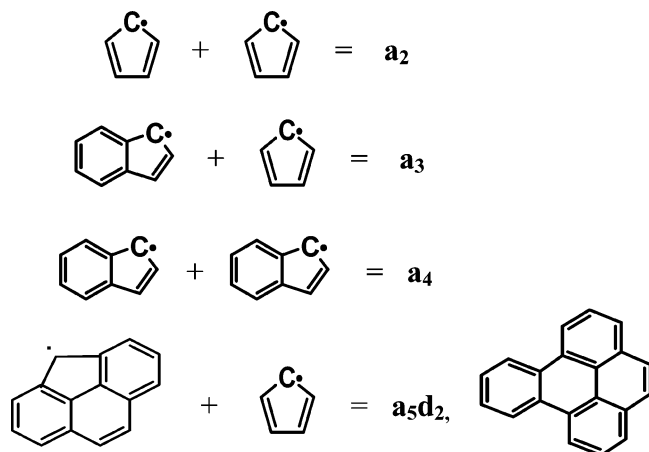
On the other hand, methyl-substituted PAHs produced from methyl radical attack at single and double fusing sites, for example, methylnaphthalene or methylpyrene also form their corresponding radicals at high temperatures, which further changed to PAHs with three- and four-membered rings by H_2 elimination and ring closing processes such as
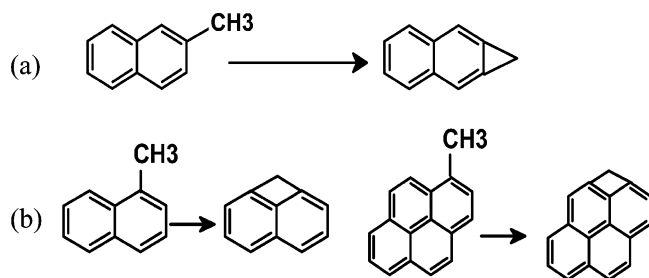
These resulting PAHs having three- or four-membered rings contain only single and double fusing sites due to which they cannot contribute in the further ring growth process efficiently to form large PAHs. Existence of PAHs with an odd number of carbons is also proposed by Apicella et al.[19] without any

TABLE 1: Chemical Species Detected during the Pyrolysis of Toluene

mass (amu)	chemical formula	mass (amu)	chemical formula	mass (amu)	chemical formula
15	CH_3	168	$C_6H_5CH_2C_6H_5$	350	$C_{28}H_{14}$
28	C_2H_4	176	$C_2HC_{10}H_6C_2H$	352	$C_{28}H_{16}$
40	C_3H_4	178	$C_{14}H_{10}$	364	$C_{28}H_{14}CH_3$
50	C_4H_2	180	$C_{14}H_{12}$	374	$C_{30}H_{14}$
52	CH_2CHCCH	182	$C_{14}H_{14}$	376	$C_{30}H_{16}$
66	c-C_5H_6	190	$C_{15}H_{10}$	390	$C_{30}H_{15}CH_3$
78	C_6H_6	192	$C_{14}H_9CH_3$	398	$C_{32}H_{14}$
79	c-$C_5H_5CH_3$	202	$C_{16}H_{10}$	400	$C_{32}H_{16}$
91	$C_6H_5CH_2$	204	$C_{16}H_{12}$	402	$C_{32}H_{18}$
92	$C_6H_5CH_3$	216	$C_{16}H_9CH_3$	414	$C_{32}H_{15}CH_3$
102	$C_6H_5C_2H$	226	$C_{18}H_{10}$	424	$C_{34}H_{16}$
104	$C_6H_5C_2H_3$	228	$C_{18}H_{12}$	426	$C_{34}H_{18}$
106	$C_6H_5C_2H_5$ or	230	$C_{20}H_{10}$	438	$C_{34}H_{15}CH_3$
	$CH_3C_6H_4CH_3$	242	$C_{18}H_{11}CH_3$	448	$C_{36}H_{16}$
115	C_9H_7	252	$C_{20}H_{12}$	450	$C_{36}H_{18}$
116	C_9H_8	254	$C_{20}H_{14}$	464	$C_{36}H_{17}CH_3$
126	$C_2HC_6H_4C_2H$	266	$C_{20}H_{11}CH_3$	472	$C_{38}H_{16}$
127	$C_{10}H_7$	276	$C_{22}H_{12}$	474	$C_{38}H_{18}$
128	$C_{10}H_8$	278	$C_{22}H_{14}$	486	$C_{38}H_{15}CH_3$
130	$C_{10}H_{10}$	290	$C_{22}H_{11}CH_3$	496	$C_{40}H_{16}$
140	$C_{11}H_8$	300	$C_{24}H_{12}$	498	$C_{40}H_{18}$
142	$C_{10}H_7CH_3$	302	$C_{24}H_{14}$	512	$C_{40}H_{17}CH_3$
152	$C_{10}H_6C_2H_2$	314	$C_{24}H_{11}CH_3$	520	$C_{42}H_{16}$
154	C_6H_5-C_6H_5	326	$C_{26}H_{14}$	522	$C_{42}H_{18}$
166	$C_{13}H_{10}$	340	$C_{26}H_{13}CH_3$		

mechanistic discussion. Finally the kinetic mechanisms discussed in this temperature range can be summarized as:

(a) The formation pathways of large PAHs in toluene pyrolysis are contributed by inter and intramolecular reactions of cyclopenta fused radicals, i.e., radical species with an odd number of carbon atoms.

(b) The growth of large PAHs is highly influenced by the phenyl radical attack especially on the triple fusing site of PAHs.

(c) The role of the HACA mechanism is only found important for ring growth by two carbon atoms from the PAHs containing triple fusing sites produced by the above reactions.

Chemical Kinetics in High-temperature ($>$1500 K) Region. An overview of Figures 11 and 12 gives the following information. In both cases most of the signals of species having an odd number of carbon atoms are suppressed while large PAH signals as well as signals of phenyl-PAHs [$a_n(d_m)$-a_1] completely disappeared.

On the other hand, new peaks for polyynes such as triacetylene (74 amu) and several weak peaks with mass number -2 from primary PAHs appeared.

Mass peaks at $m/z = 50$ assigned to diacetylene suddenly increased.

Detailed Interpretations and Expected Mechanisms. These peaks with -2 mass numbers are attributed to the ethynyl derivatives ($a_nd_mC_1$) and diethynyl derivatives ($a_nd_mC_2$). Particularly in both cases diacetylene, triacetylene ($m/z =$74 amu), phenyldiacetylene a_1C_2 ($m/z =$126 amu), and diacenaphthylene a_2C_2 ($m/z =$176 amu) are found to be significant. These observations support the production of acetylene in high concentrations from the decomposition of some neutral and radical species such as C_6H_6, C_6H_5, C_7H_7, and c-C_5H_5 (Figure 13) as well as provide evidence for the disappearance of phenyl PAHs and depression of methyl PAHs due to trapping of the resulting radicals (phenyl and methyl) by C_2H_2. This indicates that most of the toluene is converted into smaller species (especially acetylene) through decomposition reactions R13 and R22. The depression of large PAH growth and growth of abundance of $a_n(d_m)C_l$ species can be explained together based
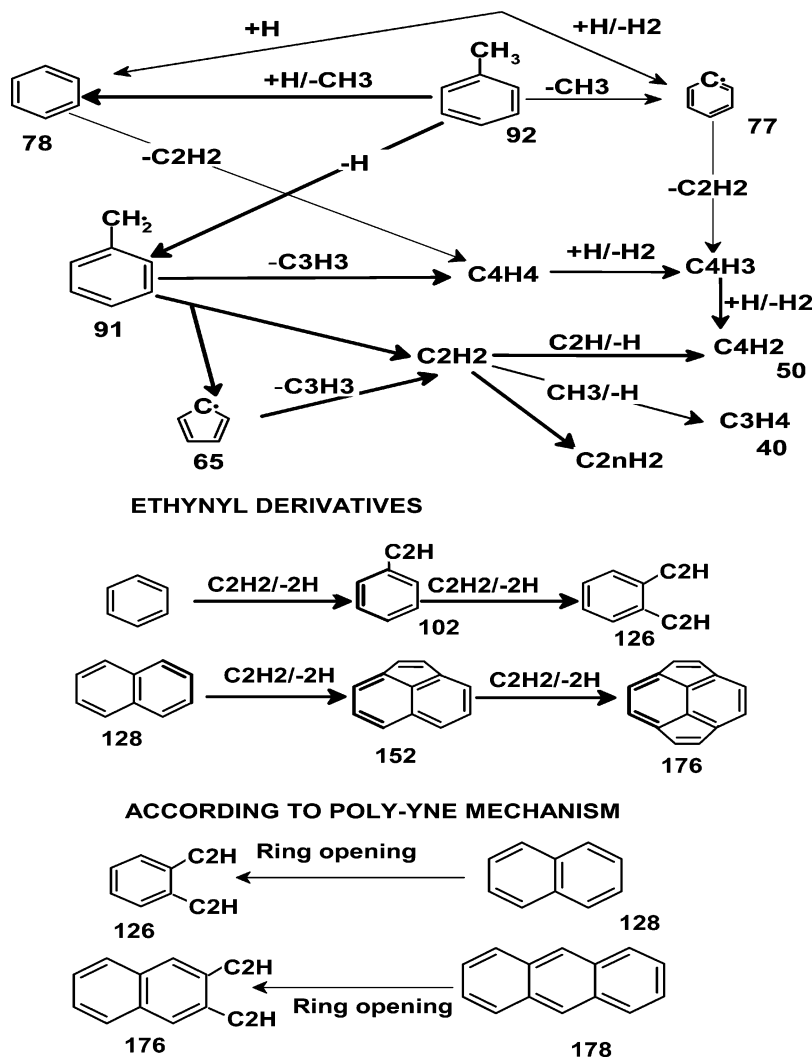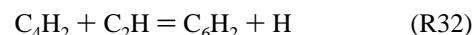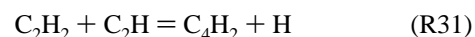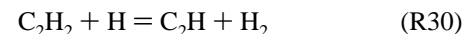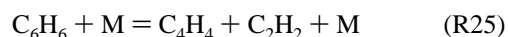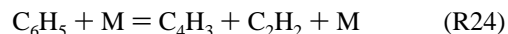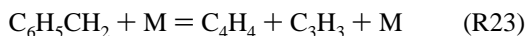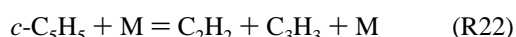
Figure 13. Formation mechanism of products of toluene pyrolysis above 1507 K dominated by the HACA mechanism and decomposition reactions. Bold arrows indicate dominant routes, and numbers represent molecular masses.

on the production of sufficient C_2H_2 from unimolecular decompositions, as:

1. Unstable primary (linear chain) PAHs are expected to grow to fully stable condensed (benzenoid) PAHs by the HACA. As unstable primary PAHs with zigzag structures contain triple fusing sites, they easily changed by one-step HACA to condensed PAHs having only single and double fusing sites. These resulting condensed PAHs can be easily changed into PAHs with five-membered ring by one-step HACA, which is supported by the observation of such species at this temperature.

2. Another cause of the depression of large PAHs is the trapping of the key radicals CH_3 and phenyl by C_2H_2 before attacking the small PAHs, which stops their further growth into large PAHs. This is supported by the appearance of phenylacetylene and propyne signals together with the disappearance of phenyl PAH [$a_n(d_m)$-a_1] signals.

The increase in the intensity of diacetylene (C_4H_2, 50 amu) may also be contributed by the reactions R23−R31. Diacetylene (C_4H_2)is further consumed by reaction R32 to form triacetylene (C_6H_2, $m/z = 74$ amu)

$$c\text{-}C_5H_5 + M = C_2H_2 + C_3H_3 + M \qquad (R22)$$

$$C_6H_5CH_2 + M = C_4H_4 + C_3H_3 + M \qquad (R23)$$

$$C_6H_5 + M = C_4H_3 + C_2H_2 + M \qquad (R24)$$

$$C_6H_6 + M = C_4H_4 + C_2H_2 + M \qquad (R25)$$

$$C_4H_4 + M = C_4H_2 + H_2 + M \qquad (R26)$$

$$C_4H_3 + M = C_4H_2 + H + M \qquad (R27)$$

$$C_4H_4 + H = C_4H_3 + H_2 \qquad (R28)$$

$$C_4H_3 + H = C_4H_2 + H_2 \qquad (R29)$$

$$C_2H_2 + H = C_2H + H_2 \qquad (R30)$$

$$C_2H_2 + C_2H = C_4H_2 + H \qquad (R31)$$

$$C_4H_2 + C_2H = C_6H_2 + H \qquad (R32)$$
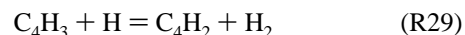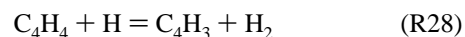
Because of the decrease in concentrations of key radicals, especially $C_6H_5CH_2$, C_6H_5, c-C_5H_5, and CH_3, the dominant routes for the formation of large PAHs cannot be accelerated enough. As a result, large PAH concentration becomes insufficient to be detected. Acetylene could not be detected in this study due to its high ionization potential (11.40 eV) greater than the ionization energy of SPI (10.5 eV) used in the present study.

According to the polyynes kinetic model,[68] diethynyl derivatives are produced by the ring-opening reactions of the closest

PAH Formation in Toluene Pyrolysis

J. Phys. Chem. A, Vol. 111, No. 34, 2007 **8323**

large PAH species by the fission of one of the C—C bonds of the aromatic ring. These ethynyl derivatives further converted to polyynes by C_2H_2 elimination following sequential reactions. On the other hand our experimental results support the formation of diethynyl derivatives by the HACA mechanism and polyynes by the above explained chain reactions. Reaction mechanisms discussed at this temperature are summarized in Figure 13. Observation of the disappearance of large PAHs at high temperatures was also reported in other studies.[13,16,30,31] Finally, it can be concluded that the kinetic mechanism in this temperature zone is dominated by the HACA mechanism.

Benzyl radical decomposition is the most important reaction in toluene pyrolysis because it decides the formation routes of products. Both reactions R13 and R23 are suggested by Colket et al.[10] and Smith et al.[30,31] for benzyl decomposition routes. On the other hand, reaction R33 is proposed by shock tube studies[25,26,28,29,58,67] and Frochtenicht et al.[69] based on a photolysis study in a molecular beam with a mass spectrometer

$$C_6H_5CH_2 = C_7H_6 + H \qquad (R33)$$
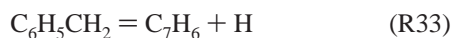
Jones et al.[67] suggested both reactions R13 and R33 based on their experimental and theoretical (especially by ab initio quantum chemical calculations) results. Observation of mass peaks for cyclopentadiene (c-C_5H_6), vinylacetylene (C_4H_4), and diacetylene (C_4H_2) in the present study indicates the decomposition of the benzyl radical by reactions R13 and R23.

Marsh et al.[20] reported that the concentration of PAHs decreases with an increase in number of aromatic rings. Thus, PAHs larger than 522 amu could not be detected in this study probably due to very low concentration. Similar to Mathieu et al.[13] and Dobbins et al.[14,15] most of our detected species masses coincide with those predicted by Stein and Fahr[82] to be the most thermodynamically stable isomers (Stabilomers). Mass spectra do not identify the species. Therefore, only sequential discussions are presented here.

Wang and Frenklach[70] modeled the kinetics of the combustion process through the network of elementary reactions for PAH formation by using the HACA mechanism. This mechanism was further supported by many other studies.[13,71−77] However, an increase in the mass of PAHs by the HACA is not sufficient to explain the very fast formation of soot in combustion processes.[10,11,30,31,62−65] The mechanism for the formation of soot precursor by aromatic radical−radical combinations and radical−molecule reactions proposed by Homann and Wagner[78] is thought to be the major path and addition of di-acetylene and acetylene as mortar to hold aromatic breaks together. The present study has found qualitative evidence for the active role of cyclopenta-fused PAH radicals and the phenyl radical in large PAH growth while the role of the HACA is found to be only significant for ring growth from triple fusing sites. Thus, it seems clear that only HACA is not sufficient to explain the fast process of soot generation.

Conclusions

The mechanistic study of toluene pyrolysis at low pressures (8.25−15.11 Torr) and temperatures (1136−1507 K) can be summarized as following:

1. Several sequences of PAHs from small to large PAHs up to mass 522 amu ($C_{42}H_{18}$), their methyl, phenyl, and ethynyl derivatives including some kinetically important radicals are detected.

2. This study confirms that any one kinetic model alone cannot explain perfectly the large PAH formation in toluene pyrolysis. The role of aromatic radical−radical and radical− molecule reactions are found to be dominant while the influence of the HACA mechanism is also important for ring growth in one step by two carbon atoms from PAHs having a triple fusing site.

3. Different reaction flow paths for the formation of PAHs are proposed on the basis of experimental results with a major emphasis on phenyl, cyclopentadienyl, benzyl, indenyl, and cyclopenta-fused PAHs radicals resulting from methyl PAHs.

References and Notes

(1) Bone W. A.; Townend D. T. A. *Flame and Combustion in Gases*; Longmans, Green and Co.: New York, 1927, p 406.

(2) Haynes, B. S; Wagner, H. G. *Prog. Energy Combust. Sci.* **1981**, 7, 229.

(3) Homann, K. H. *Proc. Combust. Inst.* **1984**, *20*, 857.

(4) Howard J. B. *Proc. Combust. Inst.* **1990**, *23*, 1107.

(5) *Soot Formaiton in Combustion: Mechanisms and Models*; Bockhorn, H., Ed.; Springer-Verlag: Berlin, 1994.

(6) Glassman, I. *Combustion*; Academic Press: San Diego, CA, 1996.

(7) Frenklach M. *Phys. Chem. Chem. Phys.* **2002**, *4*, 2028−2037.

(8) Schuetz, C. A; Frenklach, M. *Proc. Combust. Inst.* **2002**, *29*, 2307− 2314.

(9) Skjoth-Rasmussen, M. S.; Glarborg, P.; Ostberg, M.; Johannessen, J. T.; Livbjerg, H.; Jensen, A. D; Christensen, T. S. *Combust. Flame* **2004**, *136*, 91−128.

(10) Colket, M. B; Seery, D. J. *Proc. 25th combust. Inst* **1994**, 883− 891.

(11) Mukherjee, J.; Sarofim, A. F; Longwell, J. P. *Combust. Flame* **1994**, *96*, 191−200.

(12) Bockhorn et al. *Ber. Bunsen-Ges. Phys. Chem.* **1983**, *87*, 1067.

(13) Mathieu, O.; Frache, G.; Djebaili-Chaumeix, N.; Pillard, C. E.; Krier, G.; Muller, J. F.; Douce, F.; Manuelli, P. *Proc. Combust. Inst.* **2006**, *31*, 511−519.

(14) Dobbins, R. A.; Fletcher, R. A; Chang, H. C. *Combust. Flame* **1998**, *115*, 285−298.

(15) Dobbins, R. A.; Fletcher, R. A; Lu, W. *Combust. Flame* **1995**, *100*, 301−309.

(16) Keller, A.; Kovacs, R.; Homann, K.-H. *Phys. Chem. Chem. Phys.* **2002**, *2*, 1667−1675.

(17) Kent, J. H; Wagner, H. G. *Proc. Combust. Inst.* **1984**, *19*, 1007− 1015.

(18) Lafleur, A. L.; Taghizadeh, K.; Howard, J. B.; Anacleto, J. F; Quilliam, M. A. *J. Am. Soc. Mass Spectrom.* **1996**, *7*, 276−286.

(19) Apicella, B; Carpentieri, A.; Alfe, M.; Barbella, R.; Tregrossi, A.; Pucci, P.; Ciajolo, A. *Proc. Combust. Inst.* **2006**, *31*, 547−553.

(20) Marsh, N. D.; Ledesma, E. B.; Wornat, M. J.; Tan, M. P.; Zhu, D.; Law, C. K. *Polycyclic Aromat. Compd.* **2005**, *25*, 227−244.

(21) Eng, R. A.; Gebert, A.; Goos, E.; Hippler, H.; Kachiani, C. *Phys. Chem. Chem. Phys.* **2002**, *4*, 3989−3996.

(22) Pamidimukkala, K. M.; Kern, R. D.; Patel, M. R.; Kiefer, J. H. *J. Phys. Chem.* **1987**, *91*, 2148−2154.

(23) Berthelot, M. *Ann. Chem. Phys.* **1866**, *9*, 471.

(24) Szwarc, M. *J. Chem. Phys.* **1948**, *16*, 128−136.

(25) Astholz, D. C.; Durant, J.; Troe, J. *Proc. Combust. Inst.* **1981**, *18*, 885.

(26) Braun-Unkhoff, M.; Frank, P.; Just, T. H. *Proc. Combust. Inst.* **1988**, *22*, 1053−1061.

(27) Brouwer, L. D.; Muller-Markgraf, W.; Troe, J. *J. Phys. Chem.* **1988**, *92*, 4905−4914.

(28) Rao, V. S.; Skinner, G. B. *J. Phys. Chem.* **1989**, *93*, 1864.

(29) Hippler, H.; Reihs, C.; Troe, J. J. *Z. Phys. Chem. Neue Folge* **1990**, *167*, 1−16.

(30) Smith, R. D. *J. Phys. Chem.* **1979**, *83*, 12, 1553−1563.

(31) Smith, R. D. *Combust. Flame* **1979**, *35*, 179−190.

(32) Benson, S. W.; Buss, J. H. *J. Phys. Chem.* **1957**, *61*, 104.

(33) Harrison, A. G.; Kebarie, P.; Lossing, F. P. *J. Am. Chem. Soc.* **1961**, *83*, 777.

(34) Brooks, C. T.; Cummins, C. P. R.; Peacock, S. J. *Trans. Faraday Soc.* **1971**, *67*, 3265.

(35) Takenaka, J.; Endo, H.; Mikuni, H.; Takahashi, M. *Bull. Chem. Soc. Jpn.* **1967**, *40*, 1613−1616.

(36) Takeuchi, T.; Sakaguchi, M.; Togashi, Y. *Bull. Chem. Soc. Jpn.* **1966**, *39*, 1437−11439.

(37) Meyer, R. A.; Burr, J. B. *J. Am. Chem. Soc.* **1963**, *85*, 478.

(38) Badger, G. M.; Spotswood, T. M. *J. Chem. Soc.* **1960**, 4420−4427.

(39) Alexious, A.; Williams, A. *Combust. Flame* **1996**, *104*, 51−65.

(40) Braekman-Danheux, C.; Delaunois, C.; Quyen, N. Cu. *Fuel Process. Technol.* **1977**, *1*, 57−64.

(41) Shivaramakrishnan, R.; Tranter, R. S.; Brezinsky, K. *Combust. Flame* **2004**, *139*, 340−350.

(42) Shivaramakrishnan, R.; Tranter, R. S.; Brezinsky, K. *Proc. Combust. Inst.* **2005**, *30*, 1165−1173.

(43) Dagaut, P.; Pengloan, G.; Ristori, A. *Phys. Chem. Chem. Phys.* **2002**, *4*, 1846−1854.

(44) Emdee, J. L.; Brenzinsky, K.; Glassman, I. *J. Phys Chem.* **1992**, *96*, 2151−2161.

(45) Bounaceur, R.; Da Costa, I.; Fournet, R.; Billaud, F.; Battin-Leclerc, F. *Int. J. Chem. Kinet.* **2005**, *37*, 25−49.

(46) Davis, S. G.; Wang, H.; Brezinsky, K.; Law, C. K. *Proc. Combust. Inst.* **1996**, *26*, 1025−1033.

(47) Davis, S. G.; Law, C. K. *Combust. Sci. Technol.* **1998**, *140*, 1−6,-427−449.

(48) Shivaramakrishnan, R.; Tranter, R. S.; Brezinsky, K. *J. Phys. Chem. A* **2006**, *110*, 9388−9399.

(49) Shivaramakrishnan, R.; Tranter, R. S.; Brezinsky, K. *J. Phys. Chem. A* **2006**, *110*, 9400−9404.

(50) Klippenstein, S. J.; Harding, L. B.; Georgievskii, Y. *Proc. Combust. Inst.* **2006**, *31*, 221−229.

(51) Agafonov, G. L.; Naydenova, I.; Vlasov, P. A.; Warnatz, J. *Proc. Combust. Inst.* **2006**, *31*, 575−583.

(52) Ingold, K. U.; Lossing, F. P. *Can. J. Chem.* **1953**, *31*, 30−41.

(53) Muhlberger, F.; Hafner, K.; Kaesdorf, S.; Ferge, T.; Zimermann, R.; *Anal. Chem.* **2004**, *76*, 6753−6764.

(54) Ferge, T.; Maguhn, J.; Hafner, K.; Muhlberger, F.; Davidovic, M.; Warnecke, R.; Zimermann, R. *Environ. Sci. Technol.* **2005**, *39*, 6, 1393−1402.

(55) Tonokura, K.; Koshi, M. *Curr. Opin. Solid State Mater. Sci.* **2002**, *6*, 479−485.

(56) Nakamur, S.; Koshi, M. *Thin Solid Films* **2006**, *26*, 501.

(57) Errede, L. A.; Cassidy, J. P. *J. Am. Chem. Soc.* **1960**, *82*, 3653.

(58) Oehlschlaeger, M. A.; Davidson, D. F.; Hanson, R. K. *J. Phys. Chem. A* **2006**, *110*, 6649−6653.

(59) Baulch, D. L.; Cobos, C. J.; Cox, R. A.; Frank, P.; Hayman, G.; Just, T. H.; Kerr, J. A.; Murrells, T.; Pilling, M. J.; Troe, J.; Walker, R. W.; Warnaz, J. *J. Phys. Chem. Ref. Data* **1994**, *23* (Suppl. 1), 847−1033.

(60) Oehlschlaeger, M. A.; Davidson, D. F.; Hanson, R. K. *Proc. Combust. Inst.* **2006**, *31*, 211−219.

(61) Muller-Markgraf, W.; Troe, J. *Proc. Combust. Inst.* **1986**, *21*, 815−824.

(62) D'Anna, A.; Violi, A. *Energy Fuels* **2005**, *19*, 79−86.

(63) D'Anna, A.; Violi, A.; D'Alessio, A.; Sarofim, A. F. *Combust. Flame* **2001**, *127*, 1995−2003.

(64) Frenklach, M.; Clary, D. W.; Gardiner, W. C., Jr.; Stein, S. E. *Proc. Combust. Inst.* **1986**, *21*, 1067−1076.

(65) Bruinsma, O. S. L.; Moulijn, J. A. *Fuel Process. Technol.* **1988**, *18*, 213−236.

(66) Lu, M.; Mulholland, J. A. *Chemosphere* **2001**, *42*, 625−633.

(67) Jones, J.; Bacskay, G. B.; Mackie, J. C. *J. Phys. Chem. A* **1997**, *101*, 7105−7113.

(68) Krestinin, A. V. *Proc. Combust. Inst.* **1998**, *27*, 1557−1563.

(69) Frochtenicht, R.; Hippler, H.; Troe, J.; Toennies, J. P. *J. Photochem. Photobiol., A* **1994**, *80*, 33.

(70) Wang, H.; Frenklach, M. *Combust. Flame* **1997**, *110*, 173−221.

(71) D'Anna, A.; Violi, A.; D'Alessio, A. *Combust. Flame* **2001**, *127*, 1995−2003.

(72) Osunsanya, T.; Prescott, G.; Seaton, A. *Occup. Environ. Med.* **2000**, *58*, 154−159.

(73) Marinov, N. M.; Pitz, J. W.; Westbrook, C. K.; Castaldi, M. J.; Senkan, S. M. *Combust. Sci. Technol.* **1996**, *116−117*, 211.

(74) Castaldi, M. J.; Marinov, N. M.; Melius, C. F.; Huang, J.; Senkan, S. M.; Pitz, W. J.; Westbrook, C. K. *Proc. Combust. Inst.* **1996**, *26*, 693.

(75) McKinnon, J. T..; Howard, J. B. *Combust. Sci. Technol.* **1990**, *74*, 175.

(76) Wen, J. Z.; Thomson, M. J.; Park, S. H.; Rogak, S. N.; Lightstone, M. F. *Proc. Combust. Inst.* **2005**, *30*, 1477−1484.

(77) Zhu, J.; Lee, K. O.; Yozgatligil, A.; Choi, M. Y. *Proc. Combust. Inst* **2005**, *30*, 2781−2789.

(78) Homann, K. H.; Wagner, H. G. *Proc. R. Soc. London, Ser. A* **1968**, *307*, 141.

(79) Colket, M. B.; Seery, D. J. *Proc. Combust. Inst.* **1994**, *25*, 883−891.

(80) McEnally, C S.; Pfefferle, L. D. *Proc. Combust. Inst.* **2000**, *28*, 2569−2576.

(81) McEnally, C. S.; Pfefferle, L. D. *Combust. Sci. Technol.* **1997**, *128*, 257−278.

(82) Stein, S. E.; Fahr, A. *J. Phys. Chem.* **1985**, *89*, 3714−3725.